Since January 2020 Elsevier has created a COVID-19 resource centre with free information in English and Mandarin on the novel coronavirus COVID-19. The COVID-19 resource centre is hosted on Elsevier Connect, the company's public news and information website.

Chaos, Solitons and Fractals 159 (2022) 112110

Contents lists available at ScienceDirect

Chaos, Solitons and Fractals

Nonlinear Science, and Nonequilibrium and Complex Phenomena

journal homepage: www.elsevier.com/locate/chaos

Review

The influence of quadratic Lévy noise on the dynamic of an SIC contagious illness model: New framework, critical comparison and an application to COVID-19 (SARS-CoV-2) case

Yassine Sabbar [a], Driss Kiouach [a], S.P. Rajasekar [b,*], Salim El Azami El-idrissi [a]

[a] LPAIS Laboratory, Faculty of Sciences Dhar El Mahraz, Sidi Mohamed Ben Abdellah University, Fez, Morocco
[b] Department of Mathematics, Government Arts College for Women, Nilakottai 624202, Tamilnadu, India

ARTICLE INFO

Article history:
Received 5 January 2022
Received in revised form 8 April 2022
Accepted 10 April 2022
Available online 25 April 2022

Keywords:
SIC epidemic model
Quadratic Lévy noise
Extinction
Ergodicity
COVID-19

ABSTRACT

This study concentrates on the analysis of a stochastic SIC epidemic system with an enhanced and general perturbation. Given the intricacy of some impulses caused by external disturbances, we integrate the quadratic Lévy noise into our model. We assort the long-run behavior of a perturbed SIC epidemic model presented in the form of a system of stochastic differential equations driven by second-order jumps. By ameliorating the hypotheses and using some new analytical techniques, we find the exact threshold value between extinction and ergodicity (*persistence*) of our system. The idea and analysis used in this paper generalize the work of N. T. Dieu et al. (*2020*), and offer an innovative approach to dealing with other random population models. Comparing our results with those of previous studies reveals that quadratic jump-diffusion has no impact on the threshold value, but it remarkably influences the dynamics of the infection and may worsen the pandemic situation. In order to illustrate this comparison and confirm our analysis, we perform numerical simulations with some real data of COVID-19 in Morocco. Furthermore, we arrive at the following results: (i) the time average of the different classes depends on the intensity of the noise (ii) the quadratic noise has a negative effect on disease duration (iii) the stationary density function of the population abruptly changes its shape at some values of the noise intensity.
Mathematics Subject Classification 2020: 34A26; 34A12; 92D30; 37C10; 60H30; 60H10.

1. Introduction

1.1. Study background

Infectious illnesses are health disruptions caused by tiny components like viruses, germs, bacteria, fungi, or parasites. These microorganisms live in and on our bodies and propagate through many ways of dissemination such as direct physical contact (*horizontal spread*), mother to baby (*vertical transfer*), airborne particles, water, food, animal, or insect bite [1]. Minor infections may respond the rest and home treatments, while life-threatening diseases may require hospitalization.

In late 2019, a deadly disease (*Coronavirus disease 2019, abbreviated as COVID-19*) obstructed ordinary lifestyles [2] and highly strained the healthcare professionals and medical structures [3]. Biologically, the great contagiousness and quick spread of this epidemic following its insertion into the host population is due to the shortage of pre-existing immunity against the virus [4]. This latter is transmitted between humans by direct contact with frequently touched objects and surfaces or by small water droplets produced by the exhalation of infected individuals [5]. Respiratory problems, change in the sense of smell or taste, fever, and dry cough represent the principal symptoms of the disease [6]. In order to partially prevent and control the spread of this epidemic, the government and its authorities have ordered everyone to wear a mask or muzzle, clean hands frequently and take measures such as general curfews, isolation and vaccination [7,8].

In mathematical biology, dynamical systems have long been employed for analyzing and understanding the behavior of diseases in the population and examining the impact of intervention strategies [9]. The SIC (*Susceptibles–Infected–Constantly recovered*) model is one of the most substantial systems in epidemiological patterns and malady control which was originally proposed and treated by Kermack and McKendrick [1] in 1927. From then on, various formulations of the SIC model with different factors have been investigated by many researchers due to their theoretical and functional value [10,11]. In this model, the overall population is typically divided into three sub-

* Corresponding author.
E-mail addresses: yassine.sabbar@usmba.ac.ma (Y. Sabbar), sekaraja.sp@gmail.com (S.P. Rajasekar).

https://doi.org/10.1016/j.chaos.2022.112110
0960-0779/

populations, susceptible $S(t)$, infectious $I(t)$, and constantly recovered $C(t)$ individuals. The SIC epidemic model is basically expressed by the following deterministic system of nonlinear differential equations:

$$\begin{cases} \mathrm{d}S(t) = \big(\Pi - \eta_d S(t) - \tau_\beta S(t) I(t)\big)\mathrm{d}t, \\ \mathrm{d}I(t) = \big(\tau_\beta I(t) S(t) - (\eta_d + \eta_\alpha + \varpi) I(t)\big)\mathrm{d}t, \\ \mathrm{d}C(t) = \big(\varpi I(t) - \eta_d C(t)\big)\mathrm{d}t, \end{cases} \tag{1.1}$$

where the positive constants Π, η_d, η_α, τ_β and ϖ are respectively the insertion or inflow average into the population, the normal death rate, the mortality rate due to the disease, the transmission rate, and the recovery rate of the infected individuals. For the simplicity of notation, we define $S^\star = \frac{\Pi}{\eta_d}$. The model (1.1) and its general shapes were extremely applied in the COVID-19 case and several authors demonstrated that the first phase of COVID-19 (*March–May 2020*) followed the SIC dynamic. For easier reference, let us quote the following works:

- In [12], Prodanov presented some novel analytical findings and numerical algorithms for parametric estimation of the SIC model (1.1) with COVID-19 data.
- In [13], the authors proposed a two-parameters SIC model and offered a general analytical solution of the model with an application to COVID-19 case.
- In [14], the authors analyzed an SIC epidemic model for COVID-19 spread with fuzzy parameters and presented an application to the case of Indonesia.

The deterministic model (1.1) offers a systematic way to investigate transmission dynamics and produce long-term predictions [9]. Based on the expression $\mathfrak{r}_0 = \tau_\beta S^\star - (\eta_d + \eta_\alpha + \varpi)$, we can analytically establish the asymptotic behavior of the epidemic. If $\mathfrak{r}_0 > 0$, then the disease persists in the population, and if $\mathfrak{r}_0 \le 0$, the disease dies out. Commonly, $\mathfrak{r}_0$ can be formulated as the basic reproduction number $\mathrm{R}_0 = \frac{\tau_\beta S^\star}{\eta_d + \eta_\alpha + \varpi}$ and we can compare this ratio with the number 1 to distinguish between the suppression and the continuation of the illness. More interesting results on the SIC model can be found in [15] where the stability properties of equilibrium are studied. It is worth noting that model (1.1) can be improved by taking into account some realistic assumptions such as randomness. We introduce this idea in the next subsection.

1.2. The role of stochasticity in biological and physical systems

Biological and physical systems are sophisticated and complex. One of the hallmarks of complexity is randomness and uncertainties, either in the reasons of a happened phenomenon or in predicting its long-run [16]. The stochastic approach highlights many hypotheses and preoccupations by investigating the dynamics of a system. For this reason, multiplicative and additive noise sources carry out a significant role in the transient dynamics of biological and physical systems [17]. Technically, if the noise level is abnormally high, the signal can be drowned out, the similar logic for biological systems where noises help reduce infection. Regarding the physical grasp of biological models, the above two types of random noise have been extensively greatly used [18–21]. Clearly, additive noise is characterized by its proactive role in the transient dynamics of dynamical systems, and multiplicative noise is accountable for noise-induced transitions [22]. In this context, Spagnolo et al. [23] studied the dynamics of an ecosystem with multiplicative noise and a stochastic interference between the species. They showed that noise plays a pivotal role in population dynamics and its presence is responsible for the generation of quasi-deterministic temporal oscillations. Furthermore, they demonstrated that noise affects the extinction of species, which confirms the role of including stochasticity. By considering white and colored noise sources, Guarcello et al. [24] analyzed the phase dynamics in ballistic graphene-based short Josephson junctions. They explored the effects of thermal and correlated fluctuations on the escape time from these metastable states in the case of the aforementioned noises. More investigation on stabilization effects of dichotomous noise on the lifetime of the superconducting state, geometric approach to quantum phase transitions, and other intriguing studies can be found in [25–30]. Concerning bio-mathematical systems, we can also show that casual and extrinsic perturbations have a considerable effect on the infection dynamic [31–41]. In [42], the author showed that due to potential environmental changes, the epidemic model parameters are exhibit atypical and stochastic fluctuations with different degrees. Subsequently, lots of studies have inserted the white noise into the corresponding deterministic setup to show the impact of the environmental disturbances on the population dynamics [43–54]. The important issue in dealing with dynamic models is the stability of their equilibrium. To this end, Chichigina et al. [55] treated the stability of a simple system subject to multiplicative one-side pulse noise with hidden periodicity. By varying the memory, the authors in [56] analyzed the random variability of the stochastic process. As an example, they studied an epidemiological model, and they established that the noise affects the time behavior of the illness.

The previously cited systems are probabilistic models with Gaussian noise and hence their solution is continuous. However, when faced with sudden environmental shocks (*earthquakes, cyclones, fires,* etc.), these disturbances can brutally affect the solution in some cases, thus breaking its continuity [57–59]. Moreover, the impact of human interventions, economic crises, and uncontrolled flow of people may have cruel consequences on epidemiological systems and this cannot be described by using differential systems driven by white noise [60–64]. Consequently, we should employ the stochastic differential equation with significant discontinuities, so-called jumps [65]. Based on some nice properties: (i) stationary and independent increments (ii) sample paths which are almost surely right continuous with left limits, Lévy processes can be applied to many concrete and real situations [54, 66–70]. To depict this randomness, Zhang and Wang in [57] proposed the following SIC epidemic model with Lévy perturbation:

$$\begin{cases} \mathrm{d}S(t) = \big(\Pi - \eta_d S(t) - \tau_\beta S(t) I(t)\big)\mathrm{d}t + \mathrm{d}\mathcal{A}_1(t), \\ \mathrm{d}I(t) = \big(\tau_\beta I(t) S(t) - (\eta_d + \eta_\alpha + \varpi) I(t)\big)\mathrm{d}t + \mathrm{d}\mathcal{A}_2(t), \\ \mathrm{d}C(t) = \big(\varpi I(t) - \eta_d C(t)\big)\mathrm{d}t + \mathrm{d}\mathcal{A}_3(t), \end{cases} \tag{1.2}$$

where

$$\begin{aligned} \mathrm{d}\mathcal{A}_1(t) &= \overbrace{S(t)\xi_{11}\mathrm{d}\mathbb{W}_1(t)}^{\text{White noise part}} + \overbrace{\int_{\mathcal{H}} S(t_-)\chi_{11}(u)\mathbb{L}(\mathrm{d}t,\mathrm{d}u)}^{\text{Jumps noise part}}, \\ \mathrm{d}\mathcal{A}_2(t) &= I(t)\xi_{21}\mathrm{d}\mathbb{W}_2(t) + \int_{\mathcal{H}} I(t_-)\chi_{21}(u)\mathbb{L}(\mathrm{d}t,\mathrm{d}u), \\ \mathrm{d}\mathcal{A}_3(t) &= C(t)\xi_{31}\mathrm{d}\mathbb{W}_3(t) + \int_{\mathcal{H}} C(t_-)\chi_{31}(u)\mathbb{L}(\mathrm{d}t,\mathrm{d}u). \end{aligned}$$

To describe the stochastic components of this system, we consider firstly a probability triple $(\Omega,\mathscr{E},\mathbb{P})$ and an increasing, right continuous filtration $\{\mathscr{E}_t\}_{t\ge 0}$ with the fact that $\mathscr{E}_0$ includes all $\mathbb{P}$-null sets. Then, we present the following definitions:

- The left limits of $S(t)$, $I(t)$ and $C(t)$ are denoted by $S(t_-)$, $I(t_-)$, $C(t_-)$.
- The Wiener processes $\mathbb{W}_i(t)$ $(i = 1,2,3)$ are mutually independent and defined on $(\Omega,\mathscr{E},\{\mathscr{E}_t\}_{t\ge 0},\mathbb{P})$.
- $\xi_{i1} > 0$ $(i = 1,2,3)$ are the white noise intensities.
- $\mathbb{L}$ is the compensator associated with Poisson random measure $\mathcal{N}$ and special measure $\vartheta(\cdot)$ defined on a measurable set $\mathscr{H} \subset (0,\infty)$.
- $\vartheta(\mathscr{H}) < \infty$ and $\mathbb{L}(t,\mathrm{d}u)$ is an $\{\mathscr{E}_t\}$-martingale, where $\mathcal{N}(t,\mathrm{d}u) = \mathbb{L}(t,\mathrm{d}u) + t\vartheta(\mathrm{d}u)$.
- $\mathcal{N}$ is independent to $\mathbb{W}_i$ $(i = 1,2,3)$.
- $\chi_{i1} : \mathscr{H} \to (-1,\infty)$ $(i = 1,2,3)$ are three continuous functions.

For simplicity and convenience of discussion, we let $\xi^\star = \max\{\xi_{11}^2, \xi_{21}^2, \xi_{31}^2\}$, $\chi^\star(u) = \max\{\chi_{11}(u), \chi_{21}(u), \chi_{31}(u)\}$ and $\chi_\star(u) = \min\{\chi_{11}(u), \chi_{21}(u), \chi_{31}(u)\}$. Concerning the results on the asymptotic behavior of the model (2), we cite the following works:

- In [58], the authors established the threshold of the disappearance and perseverance of the disease under the following key parametric condition

$$\eta_d > 0.5(p-1)\xi^\star + \frac{1}{p}\int_{\mathcal{H}}\left((1+\chi^\star(u))^p - 1 - p\chi_\star(u)\right)\vartheta(\mathrm{d}u), \quad p > 1. \tag{1.3}$$

- In [71], the authors provided a critical review indicating that the condition (1.3) is actually a restricted hypothesis in the sense that there are many cases where it cannot be verified. Without making (1.3), they proposed an alternative approach to determine the threshold of (1.2).
- In [72], the authors proposed a general class of Lévy-jumps perturbation by considering the system (1.2) with infinite Lévy measures $\vartheta(\mathscr{H}) = \infty$ and possible correlation between stochastic components. They established the threshold of (1.2).

Lévy jumps are also used in physical domains and allow precise characterization of random processes with some discontinuities. In [73], Guarcello et al. explored the effects of Lévy noise on the dynamics of sine-Gordon solitons in long Josephson junctions. In [74], the authors investigated the influence of Gaussian and non-Gaussian noises on the ballistic graphene-based small Josephson junctions. Notably, they provided a comparative study and some useful outcomes.

1.3. Stochastic SIC system with quadratic Lévy perturbation

In this article, we introduce a generalization of the work presented in [71]. We consider a more realistic situation of the epidemics dissemination in the case of sudden environmental catastrophes and some human interventions. These disorders greatly affect the number of individuals and the random perturbation may be dependent on the square of the variables S, I, and C respectively. In view of this, we include the second-order Lévy jumps into the epidemic model (1.1) as follows:

$$\begin{cases} \mathrm{d}S(t) = \left(\Pi - \eta_d S(t) - \tau_\beta S(t)I(t)\right)\mathrm{d}t + \mathrm{d}\mathcal{P}_1(t), \\ \mathrm{d}I(t) = \left(\tau_\beta I(t)S(t) - (\eta_d + \eta_\alpha + \varpi)I(t)\right)\mathrm{d}t + \mathrm{d}\mathcal{P}_2(t), \\ \mathrm{d}C(t) = \left(\varpi I(t) - \eta_d C(t)\right)\mathrm{d}t + \mathrm{d}\mathcal{P}_3(t), \end{cases} \tag{1.4}$$

where

$$\begin{aligned} \mathrm{d}\mathcal{P}_1(t) &= \overbrace{\left(\xi_{11}S(t) + \xi_{12}S^2(t)\right)\mathrm{d}\mathbb{W}_1(t)}^{\text{Quadratic white noise part}} + \overbrace{\int_{\mathcal{H}}\left(\chi_{11}(u)S(t_-) + \chi_{12}(u)S^2(t_-)\right)\mathbb{L}(\mathrm{d}t,\mathrm{d}u)}^{\text{Quadratic jumps noise part}}, \\ \mathrm{d}\mathcal{P}_2(t) &= \left(\xi_{21}I(t) + \xi_{22}I^2(t)\right)\mathrm{d}\mathbb{W}_2(t) + \int_{\mathcal{H}}\left(\chi_{21}(u)I(t_-) + \chi_{22}(u)I^2(t_-)\right)\mathbb{L}(\mathrm{d}t,\mathrm{d}u), \\ \mathrm{d}\mathcal{P}_3(t) &= \left(\xi_{31}C(t) + \xi_{32}C^2(t)\right)\mathrm{d}\mathbb{W}_3(t) + \int_{\mathcal{H}}\left(\chi_{31}(u)C(t_-) + \chi_{32}(u)C^2(t_-)\right)\mathbb{L}(\mathrm{d}t,\mathrm{d}u). \end{aligned}$$

Here, $\xi_{i1} > 0$ $(i = 1,2,3)$ denote the Brownian motions intensities of the linear stochastic perturbation, and $\xi_{i2} > 0$ $(i = 1,2,3)$ stand for the intensities of the quadratic case. We assume that the positive quantities $\chi_{ij}(u)$ $(i = 1,2,3,\ j = 1,2)$ are continuous functions and satisfy the following main criterion

$$(\mathrm{A}): \quad \int_{\mathcal{H}}\chi_{ij}^2(u)\vartheta(\mathrm{d}u) < \infty, \quad i = 1,2,3, \quad j = 1,2. \tag{1.5}$$

Set $\mathbb{R}^{3,\star}_+ = \{(x,y,z) : x > 0, y > 0, z > 0\}$ and assume that (A) holds, then by using the same arguments presented in ([57], Theorem 1), we can readily prove that for any initial data $(S(0),I(0),C(0)) \in \mathbb{R}^{3,\star}_+$, there exists a unique, global and positive solution $(S(t),I(t),C(t)) \in \mathbb{R}^{3,\star}_+$. That is to say that the system (1.4) is well-posed biologically and mathematically.

Remark 1.1. Clearly, the dynamic of the third compartment has no impact on the behavior of model (1.4), So we can only consider the following reduced model:

$$\begin{cases} \mathrm{d}S(t) = \left(\Pi - \eta_d S(t) - \tau_\beta S(t)I(t)\right)\mathrm{d}t + \mathrm{d}\mathcal{P}_1(t), \\ \mathrm{d}I(t) = \left(\tau_\beta I(t)S(t) - (\eta_d + \eta_\alpha + \varpi)I(t)\right)\mathrm{d}t + \mathrm{d}\mathcal{P}_2(t). \end{cases} \tag{1.6}$$

In this case, we define $\mathbb{R}^{2,\star}_+ = \{(x,y) : x > 0, y > 0\}$ and we merely examine the asymptotic behavior of the susceptible and infected compartments.

1.4. Problematic and methodology

Similar to the deterministic framework, the main objective of exploring the dynamic of the disturbed epidemic models is to establish the conditions which guarantee the extinction and the permanence of the infection. Since the stochastic model (1.6) is perturbed by a quadratic stochastic perturbation, the threshold analysis is not only a complicated but also an intriguing question. In addition, Liu et al. [75] in 2017 indicated that the quadratic stochastic disturbance will be studied in the future due to technical difficulties and the feasibility of the system in mathematical epidemiology. Recently, some authors have analyzed the dynamical behavior of epidemic models with white noises in the quadratic form (*see for example*, [76–79]). To the best of our knowledge, to this day, stochastic epidemic systems with quadratic Lévy jumps perturbation have not been treated due to their complexity. In this paper, we try to deal with the extinction of the infection and the existence of a single stationary distribution (*stochastic positive equilibrium state*) of system (1.6). Roughly speaking, ergodic stationary distribution means the permanence of the epidemic. In the literature, one of the standard approaches to prove ergodicity is the Lyapunov-candidate-function, which provides just sufficient conditions in the majority of cases [80,81]. Thus, the main problematic of this article can be stated as follows:

- Is it possible to provide the sufficient and necessary condition for the ergodic property of the system (1.6) and illness extinction under only (A) without adding more assumptions?

Accurately, this current study proposes a novel method to deal with stochastic models driven by quadratic Lévy jumps. We present the enough and almost requisite criterion for the extinction of the epidemic and the ergodic property of the model (1.6). Based on some nice properties of an auxiliary equation with quadratic jump-diffusion, we establish the exact expression of the threshold $\mathcal{T}_0^\star$. In other words, if $\mathcal{T}_0^\star < 0$, then the number of infected individuals will quickly converge to zero, and if $\mathcal{T}_0^\star > 0$, then system (1.6) admits a single stationary ergodic distribution. To examine the effect of the nonlinear jump-diffusion, we illustrate its impact on the threshold value $\mathcal{T}_0^\star$ and generally on the asymptotic behavior of the epidemic.

The remnant of this study follows the following planning: in the second part, we present some asymptotic properties of an auxiliary equation with quadratic jump-diffusion, then we introduce the value of $\mathcal{T}_0^\star$. In Section 3, we prove that $\mathcal{T}_0^\star$ is the threshold of the stochastic model (1.6). In Section 4, numerical examples are introduced to highlight and emphasize our theoretical outcomes.

2. Some results on auxiliary equation with quadratic Lévy noise

In this section, we will briefly present some characteristics and properties of the model in the case of no infection. For this reason, we consider this auxiliary equation

$$\begin{cases} \mathrm{d}\Phi(t) = (\Pi - \eta_d\Phi(t))\mathrm{d}t + \left(\xi_{11}\Phi(t) + \xi_{12}\Phi^2(t)\right)\mathrm{d}\mathbb{W}_1(t) + \int_{\mathcal{H}}\left(\chi_{11}(u)\Phi(t_-) + \chi_{12}(u)\Phi^2(t_-)\right)\mathbb{L}(\mathrm{d}t,\mathrm{d}u), \\ \Phi(0) = S(0) > 0. \end{cases} \tag{2.1}$$

The following two properties can be proven effortlessly:

- The Eq. (2.1) is well posed, that is to say that for any initial data $\Phi(0) > 0$, (2.1) has a unique positive and global solution.
- By the stochastic comparison theorem [82], we deduce that $S(t) \le \Phi(t)$ for any $t \ge 0$ almost surely (briefly, a.s.).

To proceed further, we start with the following estimation.

Lemma 2.1. For any $q \in (0,1]$, there exists a constant $\widetilde{\mathfrak{m}}$ independent of $\Phi(0)$ such that

$$\limsup_{t\to\infty} \mathbb{E}\left[q^{-1}(1+\Phi)^q\right] \le \widetilde{\mathfrak{m}} < \infty. \tag{2.2}$$

Proof. We choose the Lyapunov-candidate-function $V(\Phi) = q^{-1}(1+\Phi)^q$, and we apply the operator $\mathscr{L}V$ related with (2.1). Then, we get

$$\begin{aligned} \mathscr{L}V(\Phi) &= (1+\Phi)^{q-1}(\Pi - \eta_d\Phi) + 0.5(q-1)(1+\Phi)^{q-2}\left(\xi_{11}\Phi + \xi_{12}\Phi^2\right)^2 \\ &\quad + \int_{\mathcal{H}}\left(q^{-1}\left((1+\Phi) + \chi_{11}(u)\Phi + \chi_{12}(u)\Phi^2\right)^q - q^{-1}(1+\Phi)^q - (1+\Phi)^{q-1}\left(\chi_{11}(u)\Phi + \chi_{12}(u)\Phi^2\right)\right)\vartheta(\mathrm{d}u). \end{aligned}$$

For any $q \in (0,1]$, we have the following inequality

$$\int_{\mathcal{H}}\left[\left(1 + \frac{\chi_{11}(u)\Phi}{1+\Phi} + \frac{\chi_{12}(u)\Phi^2}{1+\Phi}\right)^q - 1 - q\left(\frac{\chi_{11}(u)\Phi}{1+\Phi} + \frac{\chi_{12}(u)\Phi^2}{1+\Phi}\right)\right]\vartheta(\mathrm{d}u) \le 0,$$

which implies that $\mathscr{L}V(\Phi) \le (\Pi + \eta_d)(1+\Phi)^{q-1} - \eta_d(1+\Phi)^q$. We choose $\nu_1 = q\eta_d$ and $\nu_2 = \Pi + \eta_d$, then we obtain

$$\mathscr{L}V(\Phi) \le -\nu_1 V(\Phi) + \nu_2. \tag{2.3}$$

By using the identical arguments exposed in the proof of Lemma 2.3 in [83], we have

$$\limsup_{t\to\infty} \mathbb{E}\left[q^{-1}(1+\Phi)^q\right] \le \frac{\nu_2}{\nu_1} = \widetilde{\mathfrak{m}} < \infty.$$

Thus, we get (2.2).

Remark 2.1. If we consider only the white noise perturbation (see for example [78,79]), then we can find the stationary distribution expression of the auxiliary process (2.1). But, this expression or formula does not exist in the case of the linear Lévy jumps and even in the quadratic case. This matter is recently indicated in [84] as an open question, and the authors gave the threshold analysis of their model with an obscure stationary distribution formula. In this study, we suggest an alternate method to get the precise expression of the threshold parameter. This fresh idea that we offer is presented in the following lemma.

Lemma 2.2. The Eq. (2.1) admits a unique ergodic stationary distribution $\pi^\star(\cdot)$. Moreover, one derives from the ergodic theorem [85] that

$$\lim_{t\to\infty}\frac{1}{t}\int_0^t \Phi(s)\mathrm{d}s = \int_0^\infty x\pi^\star(\mathrm{d}x) = S^\star. \tag{2.4}$$

Proof. As stated in [86], to prove the ergodic property of (2.1), it be sufficient to check the existence of a positive function V and constants $\nu_1,\ \nu_2 > 0$, such that

$$\mathscr{L}V(\Phi) \le -\nu_1 V(\Phi) + \nu_2.$$

From the inequality (2.3), and Theorem 6.3 in [86], we can infer the existence and uniqueness of an ergodic stationary distribution $\pi^\star(\cdot)$ and

$$\lim_{t\to\infty}\frac{1}{t}\int_0^t \Phi(s)\mathrm{d}s = \int_0^\infty x\pi^\star(dx) \quad \text{a.s.} \tag{2.5}$$

Now, taking the mathematical expectation on the sides of (2.1), yields

$$\begin{aligned} 0 &= \lim_{t\to\infty}\frac{\mathbb{E}[\Phi(t)]}{t} = \Pi - \eta_d\lim_{t\to\infty}\frac{1}{t}\int_0^t \mathbb{E}[\Phi(s)]\mathrm{d}s = \Pi - \eta_d\mathbb{E}\left[\lim_{t\to\infty}\frac{1}{t}\int_0^t \Phi(s)\mathrm{d}s\right] \\ &= \Pi - \eta_d\mathbb{E}\left[\int_0^\infty x\pi^\star(\mathrm{d}x)\right] \quad (\text{via } (2.5)) \\ &= \Pi - \eta_d\int_0^\infty x\pi^\star(\mathrm{d}x). \end{aligned} \tag{2.6}$$

Then, we get

$$\lim_{t\to\infty}\frac{1}{t}\int_0^t \Phi(s)\mathrm{d}s = \int_0^\infty x\pi^\star(\mathrm{d}x) = \frac{\Pi}{\eta_d} = S^\star.$$

This completes the proof.

Remark 2.2. To illustrate the significance of the result (2.6), let's compare it to that of [58]. In fact, according to work [71], we can get the results in [58] without considering (1.3). Usually, this clause is widely used to prove the following long-time estimates:

1. $\lim_{t\to\infty}\frac{\Phi(t)}{t} = 0$ a.s.
2. $\lim_{t\to\infty}\frac{1}{t}\int_0^t \Phi(s)\mathrm{d}\mathbb{W}_1(s) = 0$, and $\lim_{t\to\infty}\frac{1}{t}\int_0^t \Phi^2(s)\mathrm{d}\mathbb{W}_1(s) = 0$ a.s.
3. $\lim_{t\to\infty}\frac{1}{t}\int_0^t \int (\chi_{11}(u)\Phi(s_-) + \chi_{12}(u)\Phi^2(s_-))\mathbb{L}(\mathrm{d}s,\mathrm{d}u) = 0$ a.s.

Elimination of (1.3) allows us to study the model (1.4) without restrictions or assumptions on the parameters of the model.

Remark 2.3. Lemma 2.2 takes into consideration the effect of quadratic Lévy jumps, and this makes it clearly an extended version of the results presented in ([71], Remarks 2 and 3).

Now we present the threshold value of our stochastic model (1.6) which is expressed by the following form

$$\mathcal{T}_0^\star = \tau_\beta S^\star - (\eta_d+\eta_\alpha+\varpi) - 0.5\xi_{21}^2 - \int_{\mathcal{H}}(\chi_{21}(u) - \ln(1+\chi_{21}(u)))\vartheta(\mathrm{d}u).$$

Remark 2.4. Note that without using the result (2.6), the threshold takes the following form

$$\mathcal{T}_0^\star = \tau_\beta\int_0^\infty x\pi^\star(\mathrm{d}x) - (\eta_d+\eta_\alpha+\varpi) - 0.5\xi_{21}^2 - \int_{\mathcal{H}}(\chi_{21}(u) - \ln(1+\chi_{21}(u)))\vartheta(\mathrm{d}u).$$

Since the expression of $\pi^\star$ is unknown, our alternative method offers an exact value of the threshold value of the model (1.6).

In the next section, we will show analytically that $\mathcal{T}_0^\star$ is the real threshold among suppression and tenacity of the disease.

3. Threshold analysis of the model (1.6) with quadratic Lévy noise

As stated in the introduction, the central question related to the analysis of epidemiological systems is to predict what will happen in the long term? So, the main purpose of this part is to process this query.

3.1. Extinction case

Theorem 3.1. Assume that $\mathcal{T}_0^\star < 0$. Then, the solution $(S(t),I(t))$ to system (1.6) (with any positive initial value) follows

$$\limsup_{t\to\infty}\frac{\ln I(t)}{t} \le \mathcal{T}_0^\star < 0 \quad \text{a.s.},$$

which indicates that the illness will exponentially (rapidly) extinct with probability 1. In addition, the distribution of susceptible population $S(t)$ converges weakly to the single stationary distribution $\pi^\star$ of $\Phi(t)$.

Biological signification 3.1. By Theorem 3.1, we show that:

1. If the Lyapunov characteristic quantity of infected persons is negative, then $I(t)$ exponentially tends to 0, explicitly, when the growth rate of $I(t)$ is negative, the disease should go away.
2. The distribution of the susceptible persons converges weakly to a unique stable distribution, which indicates that the $S(t)$ level eventually reaches a steady-state, meaning that $S(t)$ persists.

Proof of Theorem 3.1. Computing the Itô's formula of $\ln I(t)$ over the solution $(S(t),I(t))$ gives

$$\begin{aligned}\mathrm{d}\ln I(t) &= (\tau_\beta S(t) - (\eta_d+\eta_\alpha+\varpi) - 0.5(\xi_{21}+\xi_{22}I(t))^2\\ &+ \int_{\mathcal{H}}(\ln(1+\chi_{21}(u)+\chi_{22}(u)I(t)))\vartheta(\mathrm{d}u) - \int_{\mathcal{H}}\Big(\big(\chi_{21}(u)\\ &+\chi_{22}(u)I(t)\big)\vartheta(\mathrm{d}u)\Big)\mathrm{d}t + (\xi_{21}+\xi_{22}I(t))\mathrm{d}\mathbb{W}_2(t) + \int_{\mathcal{H}}\ln(1+\chi_{21}(u)+\chi_{22}(u)I(t_-))\mathbb{L}(\mathrm{d}t,\mathrm{d}u).\end{aligned}$$

According to the stochastic comparison result, we have

$$\begin{aligned}\mathrm{d}\ln I(t) &\le (\tau_\beta\Phi(t) - (\eta_d+\eta_\alpha+\varpi) - 0.5(\xi_{21}+\xi_{22}I(t))^2\\ &+ \int_{\mathcal{H}}(\ln(1+\chi_{21}(u)+\chi_{22}(u)I(t)))\vartheta(du) - \int_{\mathcal{H}}((\chi_{21}(u)+\chi_{22}(u)I(t)))\vartheta(\mathrm{d}u))\mathrm{d}t\\ &+ (\xi_{21}+\xi_{22}I(t))\mathrm{d}\mathbb{W}_2(t) + \int_{\mathcal{H}}\ln(1+\chi_{21}(u)+\chi_{22}(u)I(t_-))\mathbb{L}(\mathrm{d}t,\mathrm{d}u).\end{aligned}$$

We integrate both sides from 0 to t, then after dividing by t, we get

$$\begin{aligned}\frac{\ln I(t)-\ln I(0)}{t} \leq\ & \frac{\tau_\beta}{t}\int_0^t \Phi(s)\mathrm{d}s-(\eta_d+\eta_\alpha+\varpi)-0.5\xi_{21}^2-\int_{\mathscr{H}}(\chi_{21}(u)-\ln(1+\chi_{21}(u)))\vartheta(\mathrm{d}u)\\ &-\frac{\xi_{21}\xi_{22}}{t}\int_0^t I(s)\mathrm{d}s-\frac{0.5\xi_{22}^2}{t}\int_0^t I^2(s)\mathrm{d}s+\frac{1}{t}\int_0^t \xi_{21}\mathrm{d}\mathbb{W}_2(s)\\ &+\frac{1}{t}\int_0^t\int_{\mathscr{H}}\ln(1+\chi_{21}(u))\mathbb{L}(\mathrm{d}s,\mathrm{d}u)+\frac{1}{t}\int_0^t\int_{\mathscr{H}}\left[\ln\left(\frac{\chi_{22}(u)I(s)}{1+\chi_{21}(u)}+1\right)-\chi_{22}(u)I(s)\right]\vartheta(\mathrm{d}u)\mathrm{d}s\\ &+\frac{1}{t}\int_0^t \xi_{22}I(s)\mathrm{d}\mathbb{W}_2(s)+\frac{1}{t}\int_0^t\int_{\mathscr{H}}\ln\left(\frac{\chi_{22}(u)I(s_-)}{1+\chi_{21}(u)}+1\right)\mathbb{L}(\mathrm{d}s,\mathrm{d}u).\end{aligned}$$

Let

$$\begin{aligned}\mathcal{G}_1(t)&=\int_0^t \xi_{21}\mathrm{d}\mathbb{W}_2(s),\\ \mathcal{G}_2(t)&=\int_0^t\int_{\mathcal{H}}\ln(1+\chi_{21}(u))\mathbb{L}(\mathrm{d}s,\mathrm{d}u).\end{aligned}$$

The quadratic variations [87] of $\mathcal{G}_1(t)$ and $\mathcal{G}_2(t)$ are presented as follow

$$\langle\mathcal{G}_1(t),\mathcal{G}_1(t)\rangle=\xi_{21}^2 t \quad\text{and}\quad \langle\mathcal{G}_2(t),\mathcal{G}_2(t)\rangle=t\int_{\mathcal{H}}(\ln(1+\chi_{21}(u)))^2\vartheta(\mathrm{d}u).$$

According to the strong large numbers theorem for local martingales [87], we get

$$t^{-1}\ \mathcal{G}_1(t)\to 0 \quad\text{a.s.}\quad\text{and}\quad t^{-1}\ \mathcal{G}_2(t)\to 0 \quad\text{a.s.,}\quad\text{as}\quad t\to\infty.$$

Applying the exponential inequality for martingales described in [87], we obtain

$$\begin{aligned}\mathbb{P}\Bigg\{\sup_{0\leq t\leq n}\Bigg[&-0.5\int_0^t\xi_{22}^2I^2(s)\mathrm{d}s-\int_0^t\int_{\mathcal{H}}\left(\left(\frac{\chi_{22}(u)I(s)}{1+\chi_{21}(u)}\right)+\ln\left(\frac{\chi_{22}(u)I(s)}{1+\chi_{21}(u)}+1\right)\right)\vartheta(\mathrm{d}u)\mathrm{d}s\\ &+\int_0^t\xi_{22}I(s)\mathrm{d}\mathbb{W}_2(s)+\int_0^t\int_{\mathcal{H}}\ln\left(\frac{\chi_{22}(u)I(s_-)}{1+\chi_{21}(u)}+1\right)\mathbb{L}(\mathrm{d}s,\mathrm{d}u)\Bigg]\geq 2\ln n\Bigg\}\leq n^{-2}.\end{aligned}$$

Via Borel-Cantelli Lemma [87] (with the fact that $\sum_{n=1}^{\infty}n^{-2}<\infty$), we deduce that for almost ω in Ω, there exists $n_0>0$ that verifies for all $n\geq n_0$ and $t\in[n-1,n)$,

$$\int_0^t\xi_{22}I(s)d\mathbb{W}_2(s)+\int_0^t\int_{\mathcal{H}}\ln\left(\frac{\chi_{22}(u)I(s_-)}{1+\chi_{21}(u)}+1\right)\mathbb{L}(ds,du)\,2\ln n+0.5\int_0^t\xi_{22}^2I^2(s)ds+\int_0^t\int_{\mathcal{H}}\left(\left(\frac{\chi_{22}(u)I(s)}{1+\chi_{21}(u)}\right)-\ln\left(\frac{\chi_{22}(u)I(s)}{1+\chi_{21}(u)}+1\right)\right)\vartheta(du)ds.$$

Then, for all $n\geq n_0$, $t\in[n-1,n)\subseteq\mathbb{R}_+$ a.s., we get that

$$\begin{aligned}\frac{\ln I(t)-\ln I(0)}{t}\leq&\left[\frac{\tau_\beta}{t}\int_0^t\Phi(s)\mathrm{d}s-(\eta_d+\eta_\alpha+\varpi)-0.5\xi_{21}^2-\int_{\mathcal{H}}\left(\chi_{21}(u)-\ln(1+\chi_{21}(u))\right)\vartheta(\mathrm{d}u)\right]\\ &-\frac{\xi_{21}\xi_{22}}{t}\int_0^t I(s)\mathrm{d}s+\frac{1}{t}\int_0^t\int_{\mathcal{H}}\left(\left(\frac{\chi_{22}(u)I(s)}{1+\chi_{21}(u)}\right)-\chi_{22}(u)I(s)\right)\vartheta(\mathrm{d}u)\mathrm{d}s\\ &+\frac{\mathcal{G}_1(t)}{t}+\frac{\mathcal{G}_2(t)}{t}+\frac{2}{n-1}\ln n.\end{aligned}$$

Letting and taking superior limit on the both sides, we have

$$\begin{aligned}\limsup_{t\to\infty}\frac{\ln I(t)}{t}\leq&\tau_\beta\int_0^\infty x\pi^\star(\mathrm{d}x)-(\eta_d+\eta_\alpha+\varpi)-0.5\xi_{21}^2-\int_{\mathcal{H}}\Big(\chi_{21}(u)\\ &-\ln(1+\chi_{21}(u))\Big)\vartheta(\mathrm{d}u)\triangleq\mathcal{T}_0^\star<0\quad\text{a.s.}\end{aligned}$$

So, $\lim_{t\to\infty}I(t)=0$ a.s. To put it another way, the epidemic of the system (1.6) will quickly be removed, and its deterioration rate is at least $\mathcal{T}_0^\star$. Accordingly, we can conclude that: for any sufficiently small $h>0$, there are t_0 and $\Omega_h\subset\Omega$ such that the following results hold

$$\mathbb{P}(\Omega_h)>1-h,\quad\text{and}\quad\tau_\beta SI\leq\tau_\beta hI,\quad\text{for all}\ t\geq t_0,\quad\omega\in\Omega_h.$$

Now, from

$$(\Pi - \eta_d S(t) - \tau_\beta S(t)h)\mathrm{d}t + \mathrm{d}\mathcal{P}_1(t) \leq \mathrm{d}S(t) \leq (\Pi - \eta_d S(t))\mathrm{d}t + \mathrm{d}\mathcal{P}_1(t),$$

it follows that the distribution of the susceptible persons $S(t)$ converges weakly to the ergodic stationary distribution $\pi^\star(\cdot)$. The proof of the extinction theorem is finished.

3.2. Permanence case

In this subsection, we use Feller's property for Markov processes and the mutually exclusive possibilities result to establish the condition of the ergodic property of system (1.6), which can deal with the gap left by employing the Khasminskii analysis [88] used in [78,79]. Let's start with the following lemma.

Lemma 3.1. (Mutually limited possibilities lemma, [89]). We consider a stochastic process $\mathcal{X} \in \mathrm{R}^n$ that verifies the Feller property. Then, we have two possibilities:

1. a single ergodic probability measure exists, or
2. the following result is satisfied

$$\lim_{t\to\infty} \sup_{\hat{\rho}} \frac{1}{t}\int_0^t \int_{\mathbb{R}^n} \mathbb{P}(x;s,\mathcal{U})\hat{\rho}(\mathrm{d}x)\mathrm{d}s = 0, \tag{3.1}$$

for a given compact domain $\mathcal{U}\subset\mathrm{R}^n$, where $\widehat{\rho}$ is the initial distribution on $\mathbb{R}^n$ and $\mathrm{P}(x;s,\mathcal{U})$ stands for the probability of $\mathcal{X}$ belongs to $\mathcal{U}$ with $\mathcal{X}(0) = x \in \mathrm{R}^n$.

Theorem 3.2. For any initial data $(S(0),I(0)) \in \mathbb{R}_+^{2,\star}$, if $\mathcal{T}_0^\star > 0$, the solution $(S(t),I(t))$ to system (1.6) has the ergodic property and admits a unique stationary distribution $\pi(\cdot)$.

Biological signification 3.2. The stationary and ergodic properties indicate that the stochastic model (1.6) has a limiting distribution that predicts the subsistence of the illness in the future. That means that the epidemic will continue regardless of the initial situation.

Proof of Theorem 3.2. Analogous to the demonstration of the result presented in Lemma 3.2. of [90], we directly check the Feller hypothesis of the higher perturbed system (1.6). The principal intent of the following analysis is to demonstrate that (3.1) is impossible. Through using Itô's formula, one obtains

$$\begin{aligned}
\mathcal{L}(-\ln I(t)) =& -\tau_\beta S(t) + (\eta_d + \eta_\alpha + \varpi) + 0.5(\xi_{21} + \xi_{22}I(t))^2 \\
&- \int_{\mathcal{H}} \Big(\ln\big(1 + \chi_{21}(u) + \chi_{22}(u)I(t)\big) - (\chi_{21}(u) + \chi_{22}(u)I(t)) \Big) \vartheta(\mathrm{d}u) \\
=& -\tau_\beta \Phi(t) + (\eta_d + \eta_\alpha + \varpi) + 0.5\xi_{21}^2 \\
&+ \int_{\mathcal{H}} \big(\chi_{21}(u) - \ln(1 + \chi_{21}(u))\big)\vartheta(\mathrm{d}u) + \tau_\beta\Phi(t) - \tau_\beta S(t) + \xi_{21}\xi_{22}I(t) \\
&+ 0.5\xi_{22}^2 I^2(t) + \int_{\mathcal{H}} \left[\chi_{22}(u)I(t) - \ln\left(1 + \frac{\chi_{22}(u)I(t)}{1 + \chi_{21}(u)}\right)\right]\vartheta(du).
\end{aligned}$$

Hence, we have

$$\begin{aligned}
\mathcal{L}(-\ln I(t)) \leq& -\tau_\beta\Phi(t) + (\eta_d + \eta_\alpha + \varpi) + 0.5\xi_{21}^2 \\
&+ \int_{\mathcal{H}} \big(\chi_{21}(u) - \ln(1 + \chi_{21}(u))\big)\vartheta(\mathrm{d}u) + \tau_\beta(\Phi(t) - S(t)) \\
&+ \left(\xi_{21}\xi_{22} + \int_{\mathcal{H}} \chi_{22}(u)\vartheta(\mathrm{d}u)\right)I(t) + 0.5\xi_{22}^2 I^2(t).
\end{aligned} \tag{3.2}$$

On the other hand

$$\begin{aligned}
\mathcal{L}(\ln\Phi(t) - \ln S(t)) \leq& \left(\frac{\Pi}{\Phi(t)} - \frac{\Pi}{S(t)}\right) + \tau_\beta I(t) - 0.5\Big((\xi_{11} + \xi_{12}\Phi(t))^2 \\
&- (\xi_{11} + \xi_{12}S(t))^2\Big) + \int_{\mathcal{H}} \left[\ln\left(\frac{1 + \chi_{11}(u) + \chi_{12}(u)\Phi(t)}{1 + \chi_{11}(u) + \chi_{12}(u)S(t)}\right)\right. \\
&\left. - \chi_{12}(u)(\Phi(t) - S(t))\right]\vartheta(\mathrm{d}u) \leq \tau_\beta I(t) - \xi_{11}\xi_{12}(\Phi(t) - S(t)) \\
&- (\Phi(t) - S(t))\int_{\mathcal{H}} \left[\frac{\chi_{12}(u)(\chi_{11}(u) + \chi_{12}(u)S(t))}{1 + \chi_{11}(u) + \chi_{12}(u)S(t)}\right]\vartheta(\mathrm{d}u) \\
\leq& \tau_\beta I(t) - \xi_{11}\xi_{12}(\Phi(t) - S(t)).
\end{aligned} \tag{3.3}$$

By combining (3.2) and (3.3), we get

$$\begin{aligned}
&\mathcal{L}\Big(-\ln I(t)+\frac{\tau_\beta}{\xi_{11}\xi_{12}}(\ln\Phi(t)-\ln S(t))\Big)\\
&\leq -\tau_\beta\Phi(t)+(\eta_d+\eta_\alpha+\varpi)+0.5\xi_{21}^2+\int_{\mathcal{H}}\Big(\chi_{21}(u)-\ln(1+\chi_{21}(u))\Big)\vartheta(\mathrm{d}u)\\
&+\Big(\xi_{21}\xi_{22}+\int_{\mathscr{H}}\chi_{22}(u)\vartheta(\mathrm{d}u)\Big)I(t)+\frac{\tau_\beta^2}{\xi_{11}\xi_{12}}I(t)+0.5\xi_{22}^2I^2(t)\\
&=-\tau_\beta\int_0^\infty x\pi^\star(\mathrm{d}x)+(\eta_d+\eta_\alpha+\varpi)+0.5\xi_{21}^2+\int_{\mathcal{H}}\Big(\chi_{21}(u)-\ln(1+\chi_{21}(u))\Big)\vartheta(\mathrm{d}u)\\
&+\tau_\beta\Big(\int_0^\infty x\pi^\star(\mathrm{d}x)-\Phi(t)\Big)+\Big(\frac{\tau_\beta^2}{\xi_{11}\xi_{12}}+\xi_{21}\xi_{22}+\int_{\mathcal{H}}\chi_{22}(u)\vartheta(\mathrm{d}u)\Big)I(t)+0.5\xi_{22}^2I^2(t).
\end{aligned}$$

Choose a positive value $\mathfrak{m}$ verifying $\mathfrak{m}\geq\frac{1}{(\eta_d+\eta_\alpha+\varpi)}\Big(\frac{\tau_\beta^2}{\xi_{11}\xi_{12}}+\xi_{21}\xi_{22}+\int_{\mathscr{H}}\chi_{22}(u)\vartheta(\mathrm{d}u)\Big)$, and define

$$\mathcal{V}(t)=-\ln I(t)+\frac{\tau_\beta}{\xi_{11}\xi_{12}}(\ln\Phi(t)-\ln S(t))+\mathfrak{m}I(t).$$

Then, we have

$$\begin{aligned}
\mathcal{L}\mathcal{V}(t)\leq&-\tau_\beta\int_0^\infty x\pi^\star(\mathrm{d}x)+(\eta_d+\eta_\alpha+\varpi)+0.5\xi_{21}^2\\
&+\int_{\mathcal{H}}\Big(\chi_{21}(u)-\ln(1+\chi_{21}(u))\Big)\vartheta(\mathrm{d}u)+\tau_\beta\Big(\int_0^\infty x\pi^\star(\mathrm{d}x)-\Phi(t)\Big)\\
&+\mathfrak{m}\tau_\beta S(t)I(t)+0.5\xi_{22}^2I^2(t)=-\mathcal{T}_0^\star+\tau_\beta\Big(\int_0^\infty x\pi^\star(\mathrm{d}x)-\Phi(t)\Big)\\
&+\mathfrak{m}\tau_\beta S(t)I(t)+0.5\xi_{22}^2I^2(t).
\end{aligned}$$

Once again, applying Itô's formula to $p^{-1}(1+S)^p$ and $p^{-1}I^p$ for $0<p<1$, we easily derive

$$\begin{aligned}
\mathcal{L}\Big(\frac{(1+S(t))^p}{p}\Big)=&(1+S(t))^{p-1}(\Pi-\tau_\beta S(t)I(t)-\eta_dS(t))\\
&+0.5(p-1)(1+S(t))^{p-2}\Big(\xi_{11}S(t)+\xi_{12}S^2(t)\Big)^2\\
&+\int_{\mathcal{H}}\Bigg(\frac{\Big((1+S(t))+\chi_{11}(u)S(t)+\chi_{12}(u)S^2(t)\Big)^p}{p}-\frac{(1+S(t))^p}{p}\\
&-(1+S(t))^{p-1}\Big(\chi_{11}(u)S(t)+\chi_{12}(u)S^2(t)\Big)\Bigg)\vartheta(\mathrm{d}u)\\
&\leq\Pi-0.5(1-p)\xi_{12}^2S^{p+2}(t),
\end{aligned}$$

and

$$\begin{aligned}
\mathcal{L}\Big(\frac{I^p(t)}{p}\Big)=&I^{p-1}(t)(\tau_\beta S(t)I(t)-(\eta_d+\eta_\alpha+\varpi)I(t))+0.5(p-1)I^{p-2}(t)\Big(\xi_{21}I(t)+\xi_{22}I^2(t)\Big)^2\\
&+\int_{\mathcal{H}}\Bigg(\frac{\Big(I(t)+\chi_{11}(u)I(t)+\chi_{12}(u)I^2(t)\Big)^p}{p}-\frac{I^p(t)}{p}-I^p(t)(\chi_{11}(u)+\chi_{12}(u)I(t))\Bigg)\vartheta(\mathrm{d}u)\\
&\leq\tau_\beta S(t)I^p(t)-\Big((\eta_d+\eta_\alpha+\varpi)+0.5(1-p)\xi_{21}^2\Big)I^p(t)-(1-p)\xi_{21}\xi_{22}I^{p+1}(t)\\
&-0.5(1-p)\xi_{22}^2I^{p+2}(t)\leq\frac{\tau_\beta}{p+1}S^{p+1}(t)+\frac{p\tau_\beta}{p+1}I^{p+1}(t)-0.5(1-p)\xi_{22}^2I^{p+2}(t).
\end{aligned}$$

Define a C^2-function $\widetilde{\mathcal{V}}$ in the following form

$$\widetilde{\mathcal{V}}(S(t),I(t))=\mathfrak{K}\mathcal{V}(t)+\frac{(1+S(t))^p}{p}+\frac{I^p(t)}{p},$$

where $\mathfrak{K}>0$ is a sufficiently large number satisfying the following condition

$$-\mathfrak{K}\mathcal{T}_0^\star+\mathrm{C}\leq-2,$$

and

$$\begin{aligned}
\mathfrak{C}=\max\Bigg\{&\sup_{(S,I)\in\mathbb{R}_+^{2\star}}\Bigg\{\frac{\tau_\beta}{p+1}S^{p+1}-0.25(1-p)\xi_{12}^2S^{p+2}+\frac{p\tau_\beta}{p+1}I^{p+1}\\
&-0.25(1-p)\xi_{22}^2I^{p+2}+\Pi\Bigg\},1\Bigg\}.
\end{aligned}$$

In addition, it is seen that the function $\widetilde{\mathcal{V}}(S,I)$ reaches the lower bound at a point $(\underline{S},\underline{I})$ in the interior of $\mathbb{R}^2_+$, so we will deal with the non-negative C^2-function expressed by

$$\widetilde{\mathcal{V}}(S(t),I(t)) = \mathfrak{K}\mathcal{V}(t) + \frac{(1+S(t))^p}{p} + \frac{I(t)^p}{p} - \widetilde{\mathcal{V}}(\underline{S},\underline{I}).$$

Then, one can see that

$$\begin{aligned}\mathcal{L}\tilde{\mathcal{V}}(S(t),I(t)) \leq & -\mathfrak{K}\mathcal{T}_0^\star + \mathfrak{K}\mathfrak{m}\tau_\beta S(t)I(t) + 0.5\mathfrak{K}\xi_{22}^2 I^2(t) + \tau_\beta\mathfrak{K}\left(\int_0^\infty x\pi^\star(\mathrm{d}x) - \Phi(t)\right)\\ & - 0.25(1-p)\xi_{12}^2 S^{p+2}(t) - 0.25(1-p)\xi_{22}^2 I^{p+2}(t) + \Pi + \frac{\tau_\beta}{p+1}S^{p+1}(t)\\ & - 0.25(1-p)\xi_{12}^2 S^{p+2}(t) + \frac{p\tau_\beta}{p+1}I^{p+1}(t) - 0.25(1-p)\xi_{22}^2 I^{p+2}(t)\\ & = \mathcal{Z}(S(t),I(t)) + \tau_\beta\mathfrak{K}\left(\int_0^\infty x\pi^\star(\mathrm{d}x) - \Phi(t)\right).\end{aligned}$$

Now, we set up the following bounded domain

$$\mathcal{U}_\epsilon = \left\{(S,I)\in\mathbb{R}^{2,\star}_+ | \quad \epsilon \leq S \leq \epsilon^{-1}, \quad \epsilon \leq I \leq \epsilon^{-1}\right\},$$

where $0<\epsilon<1$ is a small enough constant. In the set $\mathbb{R}^{2,\star}_+\backslash\mathcal{U}_\epsilon$, we can choose ϵ sufficiently small such that the following assumptions hold

$$\mathfrak{K}\mathfrak{m}\tau_\beta\epsilon + \frac{p\mathfrak{K}\left(\mathfrak{m}\tau_\beta\epsilon + 0.5\xi_{22}^2\right)}{2+p}\left(\frac{2\mathfrak{K}\left(\mathfrak{m}\tau_\beta\epsilon + 0.5\xi_{22}^2\right)}{0.25(1-p)(2+p)\xi_{22}^2}\right)^{\frac{2}{p}} \leq 1, \tag{3.4}$$

$$\mathfrak{K}\varepsilon\left(\mathfrak{m}\tau_\beta + 0.5\xi_{22}^2\epsilon\right) + \frac{p\mathfrak{K}\mathfrak{m}\tau_\beta\epsilon}{2+p}\left(\frac{2\mathfrak{K}\mathfrak{m}\tau_\beta\epsilon}{0.25(1-p)(2+p)\xi_{12}^2}\right)^{\frac{2}{p}} \leq 1, \tag{3.5}$$

$$-\mathfrak{K}\mathcal{T}_0^\star + \mathfrak{D} - 0.25(1-p)\xi_{12}^2\epsilon^{-(2+p)} \leq -1, \tag{3.6}$$

$$-\mathfrak{K}\mathcal{T}_0^\star + \mathfrak{D} - 0.25(1-p)\xi_{22}^2\epsilon^{-(2+p)} \leq -1, \tag{3.7}$$

where

$$\begin{aligned}\mathfrak{D} = \sup_{(S,I)\in\mathbb{R}^{2,\star}_+}\Big\{ & 0.5\mathfrak{K}\mathfrak{m}\tau_\beta S^2 + 0.5\mathfrak{K}\left(\mathfrak{m}\tau_\beta + \xi_{22}^2\right)I^2 + \Pi + \frac{\tau_\beta}{p+1}S^{p+1}\\ & -0.25(1-p)\xi_{12}^2 S^{p+2} + \frac{p\tau_\beta}{p+1}I^{p+1} - 0.25(1-p)\xi_{22}^2 I^{p+2}\Big\}.\end{aligned}$$

For the convenience, we can divide $\mathbb{R}^{2,\star}_+\backslash\mathcal{U}_\varepsilon$ into four sub-domains,

$$\begin{aligned}\mathcal{U}_{\epsilon,1} &= \left\{(S,I)\in\mathbb{R}^{2,\star}_+ | \quad 0<S<\epsilon\right\}, \quad \mathcal{U}_{\epsilon,2} = \left\{(S,I)\in\mathbb{R}^{2,\star}_+ | \quad 0<I<\epsilon\right\},\\ \mathcal{U}_{\epsilon,3} &= \left\{(S,I)\in\mathbb{R}^{2,\star}_+ | \quad S>\epsilon^{-1}\right\}, \quad \mathcal{U}_{\epsilon,4} = \left\{(S,I)\in\mathbb{R}^{2,\star}_+ | \quad I>\epsilon^{-1}\right\}.\end{aligned}$$

Plainly, $\mathcal{U}_\epsilon^c = \mathbb{R}^{2,\star}_+\backslash\mathcal{U}_\epsilon = \mathcal{U}_{\epsilon,1}\cup\mathcal{U}_{\epsilon,2}\cup\mathcal{U}_{\epsilon,3}\cup\mathcal{U}_{\epsilon,4}$. In the following, we will verify that

$$\mathcal{Z}(S,I) \leq -1, \tag{3.8}$$

for any $(S,I)\in\mathcal{U}_\epsilon^c$ which is equivalent to proving it on the above four domains, respectively.

First situation: for any $(S,I)\in\mathcal{U}_{\epsilon,1}$, we use the inequality $SI\leq\epsilon I\leq\epsilon(1+I^2)$ and (3.4) to get that

$$\begin{aligned}\mathcal{Z}(S(t),I(t)) \leq & -\mathfrak{K}\mathcal{T}_0^\star + \mathfrak{K}\mathfrak{m}\tau_\beta\epsilon + \mathfrak{K}\mathfrak{m}\tau_\beta\epsilon I^2(t) + 0.5\mathfrak{K}\xi_{22}^2 I^2(t)\\ & - 0.25(1-p)\xi_{22}^2 I^{p+2}(t) + \Pi + \frac{\tau_\beta}{p+1}S^{p+1}(t)\\ & -0.25(1-p)\xi_{12}^2 S^{p+2}(t) + \frac{p\tau_\beta}{p+1}I^{p+1}(t) - 0.25(1-p)\xi_{22}^2 I^{p+2}(t)\\ & \leq -\mathfrak{K}\mathcal{T}_0^\star + \mathfrak{K}\mathfrak{m}\tau_\beta\epsilon + \frac{p\mathfrak{K}\left(\mathfrak{m}\tau_\beta\epsilon + 0.5\xi_{22}^2\right)}{2+p}\left(\frac{2\mathfrak{K}\left(\mathfrak{m}\tau_\beta\epsilon + 0.5\xi_{22}^2\right)}{0.25(1-p)(2+p)\xi_{22}^2}\right)^{\frac{2}{p}}\\ & + \mathfrak{C} \leq -1.\end{aligned}$$

Second situation: if $(S,I)\in\mathcal{U}_{\epsilon,2}$, similar to the first case, one obtains from (3.5) that

$$\begin{aligned}\mathcal{Z}(S(t),I(t))\leq&-\aleph\mathcal{T}_0^{\star}+\aleph\mathfrak{m}\tau_\beta\epsilon+0.5\aleph\xi_{22}^2\epsilon^2+\aleph\mathfrak{m}\tau_\beta\epsilon S^2(t)\\&-0.25(1-p)\xi_{12}^2S^{p+2}(t)+\Pi+\frac{\tau_\beta}{p+1}S^{p+1}(t)\\&-0.25(1-p)\xi_{12}^2S^{p+2}(t)+\frac{p\tau_\beta}{p+1}I^{p+1}(t)-0.25(1-p)\xi_{22}^2I^{p+2}(t)\\\leq&-\aleph\mathcal{T}_0^{\star}+\aleph\mathfrak{m}\tau_\beta\epsilon+0.5\aleph\xi_{22}^2\epsilon^2+\frac{p\aleph\mathfrak{m}\tau_\beta\epsilon}{2+p}\left(\frac{2\aleph\mathfrak{m}\tau_\beta\epsilon}{0.25(1-p)(2+p)\xi_{12}^2}\right)^{\frac{2}{p}}\\&+\mathfrak{C}\leq-1.\end{aligned}$$

Third situation: when $(S,I)\in\mathcal{U}_{\epsilon,3}$, we use the classical inequality $SI\leq S^2 2^{-1}+I^2 2^{-1}$, then

$$\begin{aligned}\mathcal{Z}(S(t),I(t))\leq&-\aleph\mathcal{T}_0^{\star}+0.5\aleph\mathfrak{m}\tau_\beta S^2(t)-0.25(1-p)\xi_{12}^2S^{p+2}(t)+0.5\aleph\mathfrak{m}\tau_\beta I^2(t)\\&+0.5\aleph\xi_{22}^2I^2(t)+\Pi+\frac{\tau_\beta}{p+1}S^{p+1}(t)-0.25(1-p)\xi_{12}^2S^{p+2}(t)\\&+\frac{p\tau_\beta}{p+1}I^{p+1}(t)-0.25(1-p)\xi_{22}^2I^{p+2}(t)\leq-\aleph\mathcal{T}_0^{\star}+\mathfrak{D}\\&-0.25(1-p)\xi_{12}^2\epsilon^{-(2+p)}\leq-1,\end{aligned}$$

which is established by (3.6).

Fourth situation: for any $(S,I)\in\mathcal{U}_{\varepsilon,4}$, similar to the case 3, we get by (3.7)

$$\begin{aligned}\mathcal{Z}(S(t),I(t))\leq&-\aleph\mathcal{T}_0^{\star}+0.5\aleph\mathfrak{m}\tau_\beta S^2(t)-0.25(1-p)\xi_{22}^2I^{p+2}(t)+0.5\aleph\mathfrak{m}\tau_\beta I^2(t)\\&+0.5\aleph\xi_{22}^2I^2(t)+\Pi+\frac{\tau_\beta}{p+1}S^{p+1}(t)-0.25(1-p)\xi_{12}^2S^{p+2}(t)\\&+\frac{p\tau_\beta}{p+1}I^{p+1}(t)-0.25(1-p)\xi_{22}^2I^{p+2}(t)\leq-\aleph\mathcal{T}_0^{\star}+\mathfrak{D}\\&-0.25(1-p)\xi_{22}^2\epsilon^{-(2+p)}\leq-1.\end{aligned}$$

Generally, the result (3.8) is obtained. On the other hand, we can easily show that there exists a positive value $\mathfrak{a}$ such that $\mathcal{Z}(S,I)\leq\mathfrak{a}$, for all $(S,I)\in\mathbb{R}_+^{2,\star}$. Accordingly, we get

$$\begin{aligned}&-\mathbb{E}\left[\tilde{\mathcal{V}}(S(0),I(0))\right]\leq\mathbb{E}\left[\tilde{\mathcal{V}}(S(t),I(t))\right]-\mathbb{E}\left[\tilde{\mathcal{V}}(S(0),I(0))\right]=\int_0^t\mathbb{E}\left[\mathcal{L}\tilde{\mathcal{V}}(S(s),I(s))\right]\mathrm{d}s\\&\leq\int_0^t\mathbb{E}(\mathcal{Z}(S(s),I(s)))\mathrm{d}s+\tau_\beta\aleph\ \mathbb{E}\left[\int_0^t\int_0^\infty x\pi^{\star}(\mathrm{d}x)\mathrm{d}s-\int_0^t\Phi(s)\mathrm{d}s\right].\end{aligned}$$

By using the ergodic property of $\Phi(t)$, we obtain

$$\begin{aligned}0\leq&\ \liminf_{t\to\infty}\frac{1}{t}\int_0^t\mathbb{E}[\mathcal{Z}(S(s),I(s))]\mathrm{d}s=\liminf_{t\to\infty}\frac{1}{t}\int_0^t\Big(\mathbb{E}\Big[\mathcal{Z}(S(s),I(s))1_{\{(S(s),I(s))\in\mathcal{U}_\epsilon^c\}}\Big]\\&+\mathbb{E}\left[\mathcal{Z}(S(s),I(s))1_{\{(S(s),I(s))\in\mathcal{U}_\epsilon\}}\right]\Big)\mathrm{d}s\leq\liminf_{t\to\infty}\frac{1}{t}\int_0^t\Big(-\mathbb{P}\big((S(s),I(s))\in\mathcal{U}_\epsilon^c\big)\\&+\mathfrak{a}\mathbb{P}\big((S(s),I(s))\in\mathcal{U}_\epsilon\big)\Big)\mathrm{d}s=-1+(\mathfrak{a}+1)\ \liminf_{t\to\infty}\frac{1}{t}\int_0^t\mathbb{P}\big((S(s),I(s))\in\mathcal{U}_\epsilon\big)\mathrm{d}s.\end{aligned}$$

Therefore,

$$\liminf_{t\to\infty}\frac{1}{t}\int_0^t\mathbb{P}\big((S(s),I(s))\in\mathcal{U}_\epsilon\big)\mathrm{d}s\geq\frac{1}{1+\mathfrak{a}}>0.$$

In other word, we have proved that

$$\liminf_{t\to\infty}\frac{1}{t}\int_0^t\mathbb{P}\big((S(0),I(0));s,\mathcal{U}_\epsilon\big)\mathrm{d}s\geq\frac{1}{1+\mathfrak{a}}>0,\quad\forall(S(0),I(0))\in\mathbb{R}_+^{2,\star}.$$

The proof of Theorem 3.2 is completed.

Remark 3.1. In view of Theorems 3.1 and 3.2, we conclude that quadratic jump-diffusion has no impact on the threshold of system (1.4).

4. Numerical simulations and discussion

4.1. Numerical experiments

Now, let us work out some simulations to illustrate the impact of quadratic jump-diffusion on the dynamic of an SIC epidemic model, and to infer the future of the ongoing COVID-19 pandemic under the assumption of stochasticity. Here, we apply the algorithm presented in [93] to discretize the disturbed system (1.4). By using the software Matlab2015b and the parameter values listed in Table 1, we treat the COVID-19 Morocco case till May 2021 under unexpected and higher-order fluctuations. We mention that we have combined two types of data:

Table 1
List of deterministic parameters in model (1.4).

Parameters	Test 1	Test 2	Test 3	Source
Π	1.9 day^{-1}	1.9 day^{-1}	1.9 day^{-1}	[91]
τ_β	0.23 day^{-1} *(Estimated)*	0.1015 day^{-1} *(Assumed)*	0.1 day^{-1} *(Assumed)*	–
η_d	0.35 day^{-1}	0.35 day^{-1}	0.35 day^{-1}	[92]
η_α	0.038 day^{-1}	0.038 day^{-1}	0.038 day^{-1}	[92]
ϖ	0.15 day^{-1}	0.15 day^{-1}	0.15 day^{-1}	[92]

1. Estimated values which are established using a long time series of cross-sections of actual data. We notice that, in Morocco, the COVID-19 pandemic persists up to now and the situation is relatively stable without complete extinction.
2. Assumed value (τ_β in Test 2 and Test 3) which is selected according to two criteria:
   (a) Appropriately verify the analytical result obtained in the case of extinction.
   (b) To numerically show the sharpness of our threshold.

For illustrative goals, in some cases, we simulate the model without noise (deterministic solution) besides the stochastic one, and we choose this initial condition: $(S(0),I(0),C(0)) = (0.5,0.1,0.1)$. Furthermore, we consider that the unity of time is one day and the number of individuals is expressed in ten million population. To fully understand the results of this subsection and for the convenience of the reader, we will divide it into three parts.

4.1.1. Test 1: continuation of COVID-19

For the sake of simplicity, we assume that $\vartheta(.,\mathscr{H}) = 1$ and we choose the deterministic parameter values from Table 1 (Test 1). Regarding the intensities of the noises, we select $\xi_{11} = 0.08$, $\xi_{21} = 0.02$, $\xi_{31} = 0.07$, $\xi_{12} = 0.028$, $\xi_{22} = 0.03$, $\xi_{32} = 0.02$, $\chi_{11} = 0.04$, $\chi_{21} = 0.07$, $\chi_{31} = 0.04$, $\chi_{12} = 0.01$, $\chi_{22} = 0.012$, $\chi_{32} = 0.01$. A simple calculation leads to

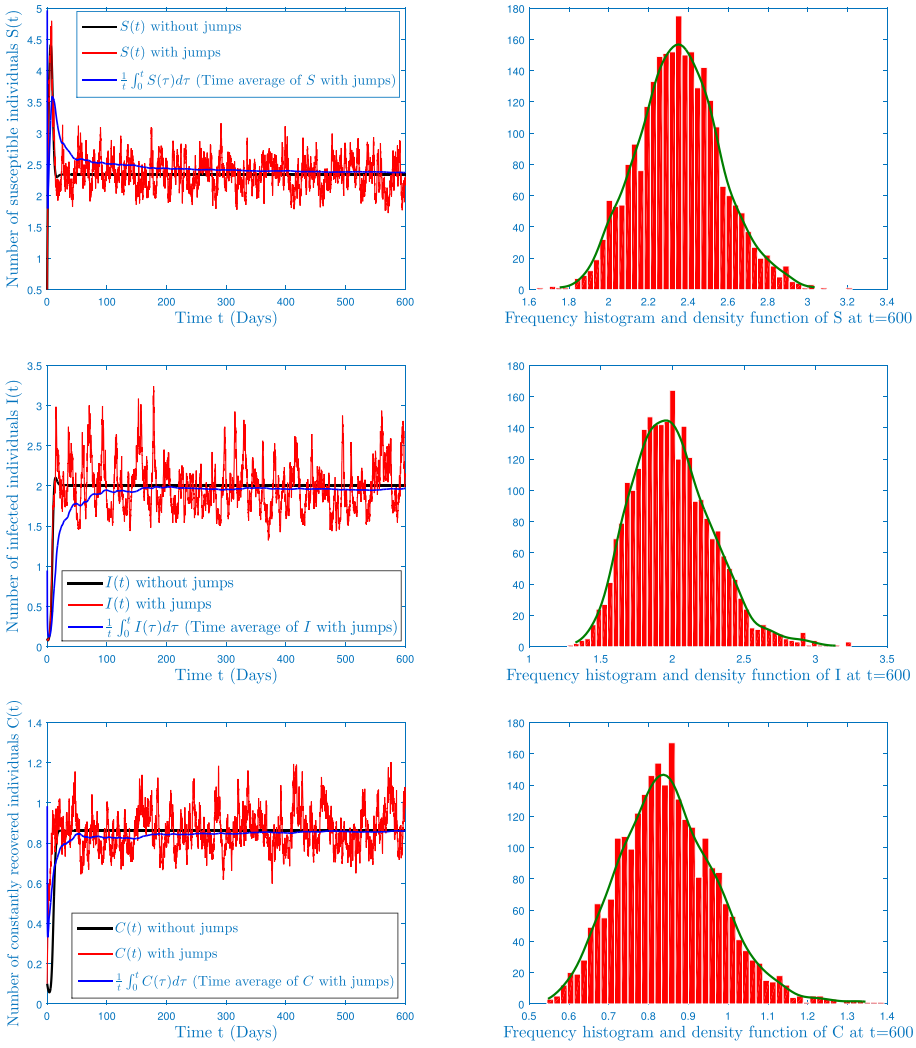

Fig. 1. The left-hand column presents the trajectories of individuals S, I and C of system (1.4) with data appearing in the second column of Table 1 - Test 1, and its deterministic system without noise, respectively. The right-hand column presents the frequency histogram fitting curves at time $t = 600$ and the theoretical density functions, respectively.

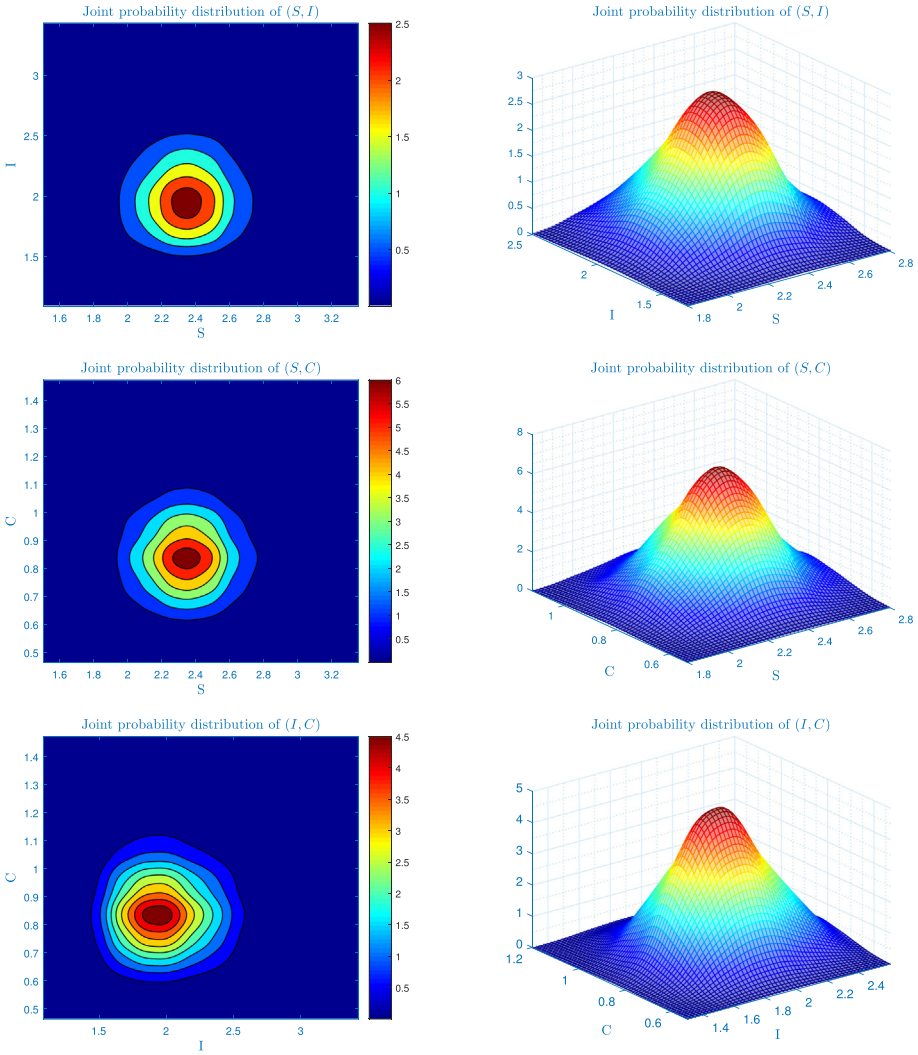

Fig. 2. The left-hand column presents the marginal two dimensional densities at time $t = 600$ of individuals S, I and C of system (1.4) with data appearing in the second column of Table 1 - Test 1, diverse colors represent distinct sizes of the density. The right-hand column presents the 3D graph of the joint 2-dimensional densities of $(S(t),I(t),C(t))$.

Table 2
Calculation of the time average of $S(t)$, $I(t)$, and $C(t)$ for different values of linear white noise intensities. The deterministic parameters are selected from Table 1 - Test 1. For other noise intensities, we select $\xi_{12} = 0.01$, $\xi_{22} = 0.01$, $\xi_{32} = 0.01$, $\chi_{11} = 0.1$, $\chi_{21} = 0.1$, $\chi_{31} = 0.1$, $\chi_{12} = 0.1$, $\chi_{22} = 0.1$, $\chi_{32} = 0.1$.

Time average	$(\xi_{11},\xi_{21},\xi_{31}) =$ (0.05,0.05,0.05)	$(\xi_{11},\xi_{21},\xi_{31}) =$ (0.1,0.1,0.1)	$(\xi_{11},\xi_{21},\xi_{31}) =$ (0.5,0.5,0.5)
$\lim_{t\to\infty} \int_0^t S(\tau)d\tau$	2.3455	2.3742 ↑	2.6281↑
$\lim_{t\to\infty} \int_0^t I(\tau)d\tau$	2.0028	1.9718 ↓	1.5536 ↓
$\lim_{t\to\infty} \int_0^t C(\tau)d\tau$	0.8603	0.8640 ↑	0.8696 ↑

Table 3
Calculation of the time average of $S(t)$, $I(t)$, and $C(t)$ for different values of quadratic white noise intensities. The deterministic parameters are selected from Table 1 - Test 1. For other noise intensities, we select $\xi_{11} = 0.01$, $\xi_{21} = 0.01$, $\xi_{31} = 0.01$, $\chi_{11} = 0.01$, $\chi_{21} = 0.1$, $\chi_{31} = 0.1$, $\chi_{12} = 0.1$, $\chi_{22} = 0.1$, $\chi_{32} = 0.1$.

Time average	$(\xi_{12},\xi_{22},\xi_{32}) =$ (0.01,0.01,0.01)	$(\xi_{12},\xi_{22},\xi_{32}) =$ (0.05,0.05,0.05)	$(\xi_{12},\xi_{22},\xi_{32}) =$ (0.1,0.1,0.1)
$\lim_{t\to\infty} \int_0^t S(\tau)d\tau$	2.3434	2.3777 ↑	2.6808 ↑
$\lim_{t\to\infty} \int_0^t I(\tau)d\tau$	2.0072	1.9660 ↓	1.4667 ↓
$\lim_{t\to\infty} \int_0^t C(\tau)d\tau$	0.8606	0.8626 ↑	0.8651 ↑

Table 4
Calculation of the time average of $S(t)$, $I(t)$, and $C(t)$ for different values of linear jumps intensities. The deterministic parameters are selected from Table 1 - Test 1. For other noise intensities, we select $\xi_{11} = 0.01$, $\xi_{21} = 0.01$, $\xi_{31} = 0.01$, $\xi_{12} = 0.01$, $\xi_{22} = 0.01$, $\xi_{32} = 0.01$, $\chi_{12} = 0.1$, $\chi_{22} = 0.1$, $\chi_{32} = 0.1$.

Time average	$(\chi_{11}, \chi_{21}, \chi_{31}) =$ (0.1,0.1,0.1)	$(\chi_{11}, \chi_{21}, \chi_{31}) =$ (0.3,0.3,0.3)	$(\chi_{11}, \chi_{21}, \chi_{31}) =$ (0.5,0.5,0.5)
$\lim_{t\to\infty} \int_0^t S(\tau)d\tau$	2.3457	2.3627 ↑	2.4824 ↑
$\lim_{t\to\infty} \int_0^t I(\tau)d\tau$	2.0061	1.9907 ↓	1.8757 ↓
$\lim_{t\to\infty} \int_0^t C(\tau)d\tau$	0.8610	0.8615 ↑	0.8622 ↑

Table 5
Calculation of the time average of $S(t)$, $I(t)$, and $C(t)$ for different values of linear jumps intensities. The deterministic parameters are selected from Table 1 - Test 1. For other noise intensities, we select $\xi_{11} = 0.01$, $\xi_{21} = 0.01$, $\xi_{31} = 0.01$, $\xi_{12} = 0.01$, $\xi_{22} = 0.01$, $\xi_{32} = 0.01$, $\chi_{11} = 0.1$, $\chi_{21} = 0.1$, $\chi_{31} = 0.1$.

Time average	$(\chi_{12}, \chi_{22}, \chi_{32}) =$ (0.1,0.1,0.1)	$(\chi_{12}, \chi_{22}, \chi_{32}) =$ (0.3,0.3,0.3)	$(\chi_{12}, \chi_{22}, \chi_{32}) =$ (0.5,0.5,0.5)
$\lim_{t\to\infty} \int_0^t S(\tau)d\tau$	2.3463	2.5503 ↑	2.9240 ↑
$\lim_{t\to\infty} \int_0^t I(\tau)d\tau$	2.0027	1.7154 ↓	1.4871 ↓
$\lim_{t\to\infty} \int_0^t C(\tau)d\tau$	0.8614	0.8636 ↑	0.8642 ↑

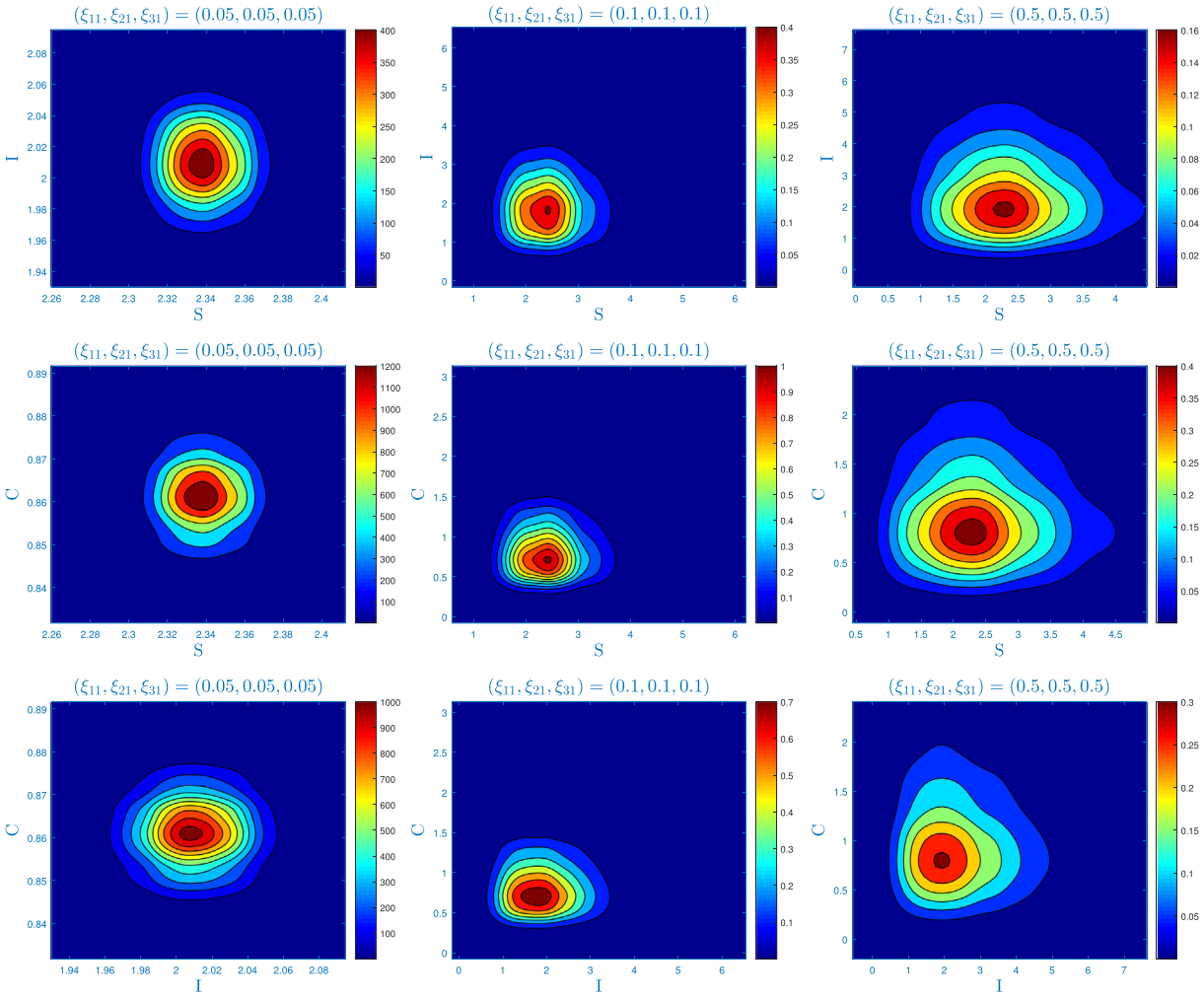

Fig. 3. Top views of the joint density functions of the solution for different values of linear white noise intensities. The deterministic parameters are selected from Table 1 - Test 1. For other noise intensities, we select $\xi_{12} = 0.028$, $\xi_{22} = 0.03$, $\xi_{32} = 0.02$, $\chi_{11} = 0.04$, $\chi_{21} = 0.07$, $\chi_{31} = 0.04$, $\chi_{12} = 0.01$, $\chi_{22} = 0.012$, $\chi_{32} = 0.01$.

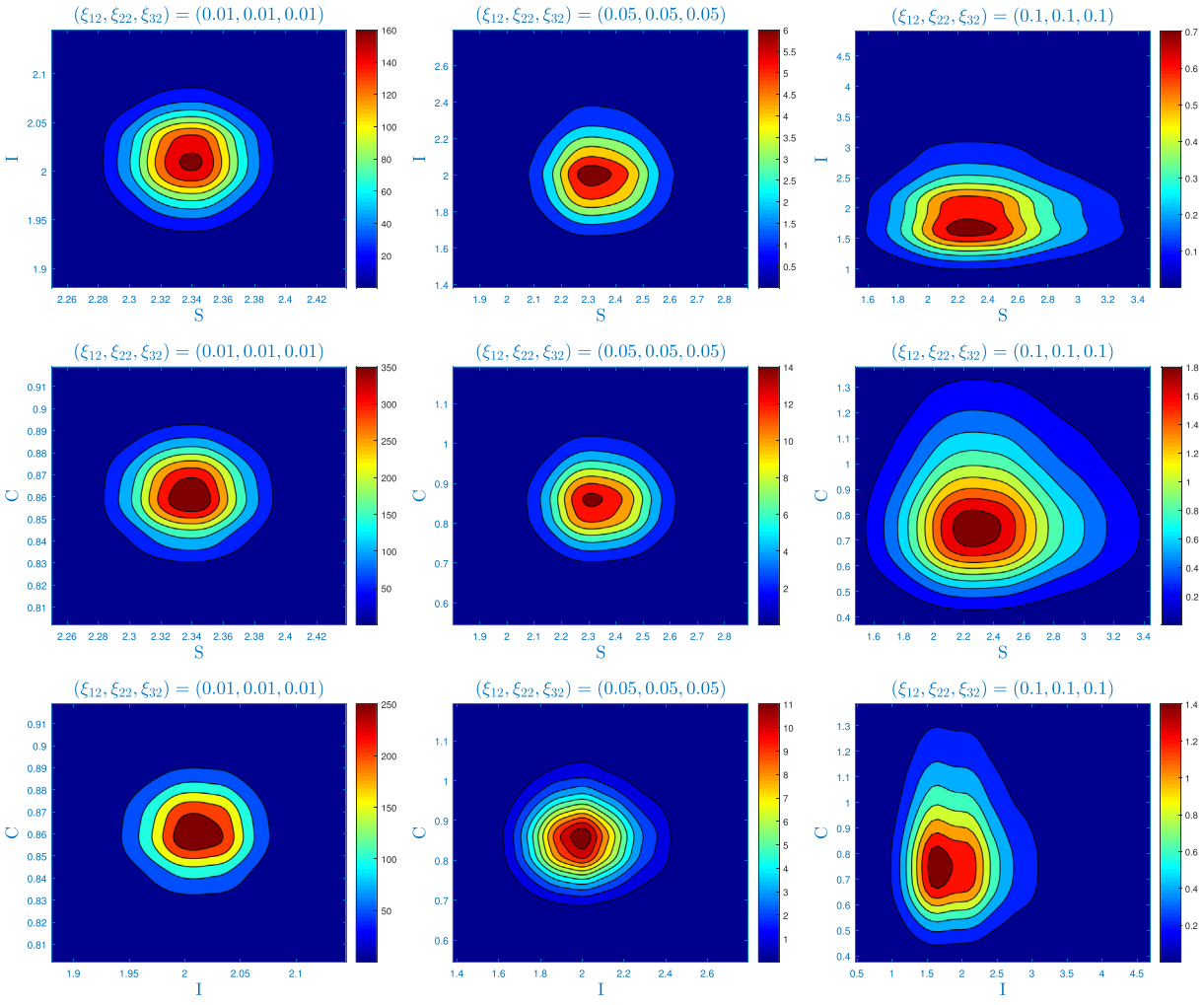

Fig. 4. Top views of the joint density functions of the solution for different values of quadratic white noise intensities. The deterministic parameters are selected from Table 1 - Test 1. For other noise intensities, we select $\xi_{11} = 0.08$, $\xi_{21} = 0.02$, $\xi_{31} = 0.07$, $\chi_{11} = 0.04$, $\chi_{21} = 0.07$, $\chi_{31} = 0.04$, $\chi_{12} = 0.01$, $\chi_{22} = 0.012$, $\chi_{32} = 0.01$.

$$\mathcal{T}_0^{\star} = \frac{\tau_\beta \Pi}{\eta_d} - (\eta_d + \eta_\alpha + \varpi) - 0.5\xi_{21}^2 - \int_{\mathrm{H}} (\chi_{21}(u) - \ln(1 + \chi_{21}(u)))\, \vartheta(\mathrm{d}u) = 0.7080 > 0.$$

Theoretical result check: since $\mathcal{T}_0^{\star}>0$, we infer from Theorem 3.2 that there is a unique ergodic stationary distribution which is depicted in Fig. 1 (see the right-hand column). Analytically, we can extract interesting information on the continuation of the processes $S(t)$, $I(t)$ and $C(t)$ which are π-integrable. Explicitly, by ergodic property, we have that

$$\lim_{t\to\infty} t^{-1} \int_0^t S(\tau)\mathrm{d}\tau = \int_{\mathbb{R}_+^{3,\star}} x\pi(\mathrm{d}x, \mathrm{d}y, \mathrm{d}z) < \infty,$$
$$\lim_{t\to\infty} t^{-1} \int_0^t I(\tau)\mathrm{d}\tau = \int_{\mathbb{R}_+^{3,\star}} y\pi(\mathrm{d}x, \mathrm{d}y, \mathrm{d}z) < \infty,$$
$$\lim_{t\to\infty} t^{-1} \int_0^t C(\tau)\mathrm{d}\tau = \int_{\mathbb{R}_+^{3,\star}} z\pi(\mathrm{d}x, \mathrm{d}y, \mathrm{d}z) < \infty.$$

Interpretation: biologically, this indicates the permanence in the mean of all classes of the population. From Fig. 1 (see left-hand column),

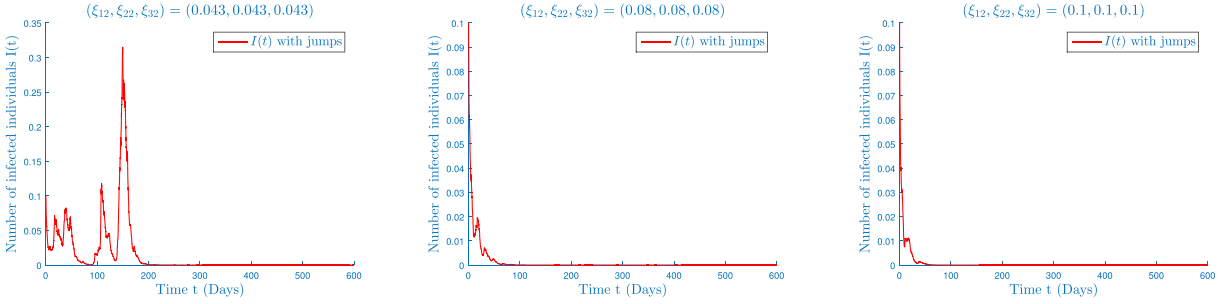

Fig. 5. Computer simulation of the trajectories $I(t)$ of system (1.4) with various values of quadratic white noise intensities. The deterministic parameters are selected from Table 1 - Test 2. For other noise intensities, we select $\xi_{11} = 0.08$, $\xi_{21} = 0.02$, $\xi_{31} = 0.07$,$\chi_{11} = 0.15$, $\chi_{21} = 0.17$, $\chi_{31} = 0.11$, $\chi_{12} = 0.075$, $\chi_{22} = 0.075$, $\chi_{32} = 0.075$.

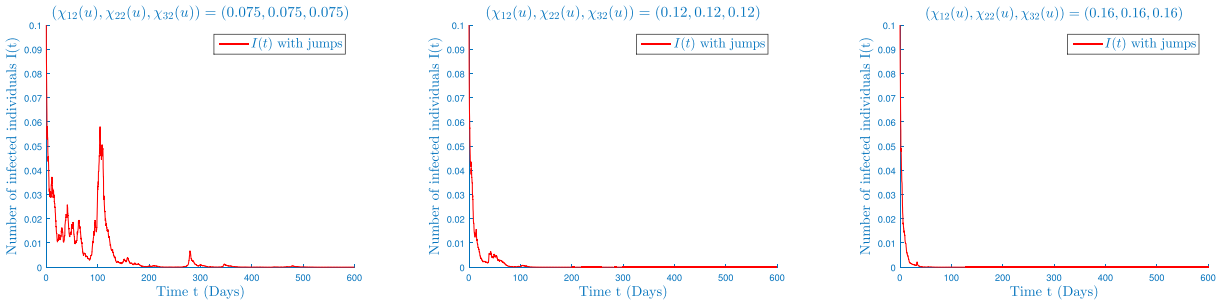

Fig. 6. Computer simulation of the trajectories $I(t)$ of system (1.4) with various values of quadratic jumps intensities. The deterministic parameters are selected from Table 1 - Test 2. For other noise intensities, we select $\xi_{11} = 0.08, \xi_{21} = 0.02, \xi_{31} = 0.07, \xi_{12} = 0.043, \xi_{22} = 0.043, \xi_{31} = 0.043, \chi_{11} = 0.15, \chi_{21} = 0.17, \chi_{31} = 0.11$.

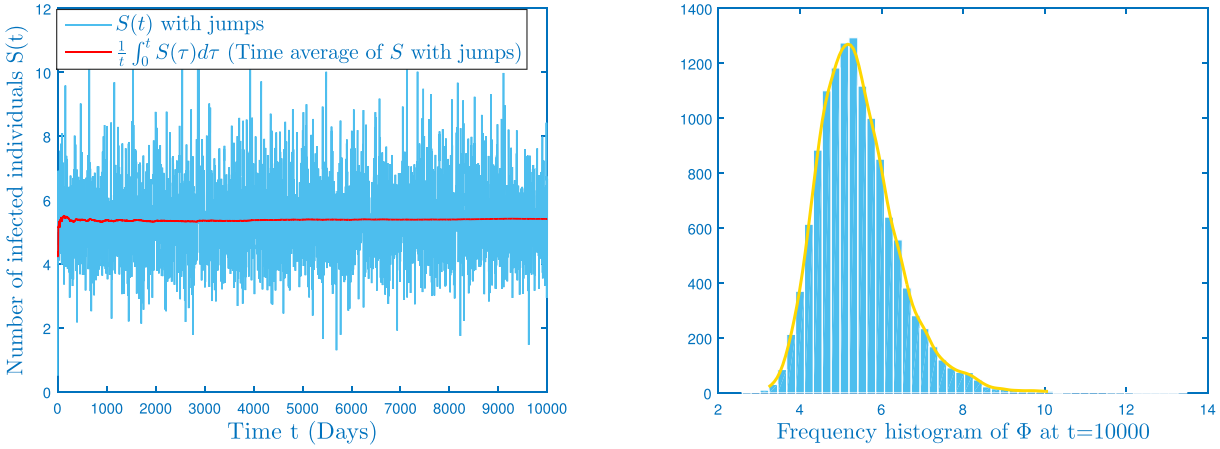

Fig. 7. Left figure: computer simulation of the path of $S(t)$. Right figure: the frequency histogram fitting curves at time $t = 10000$ of Φ and its theoretical density function.

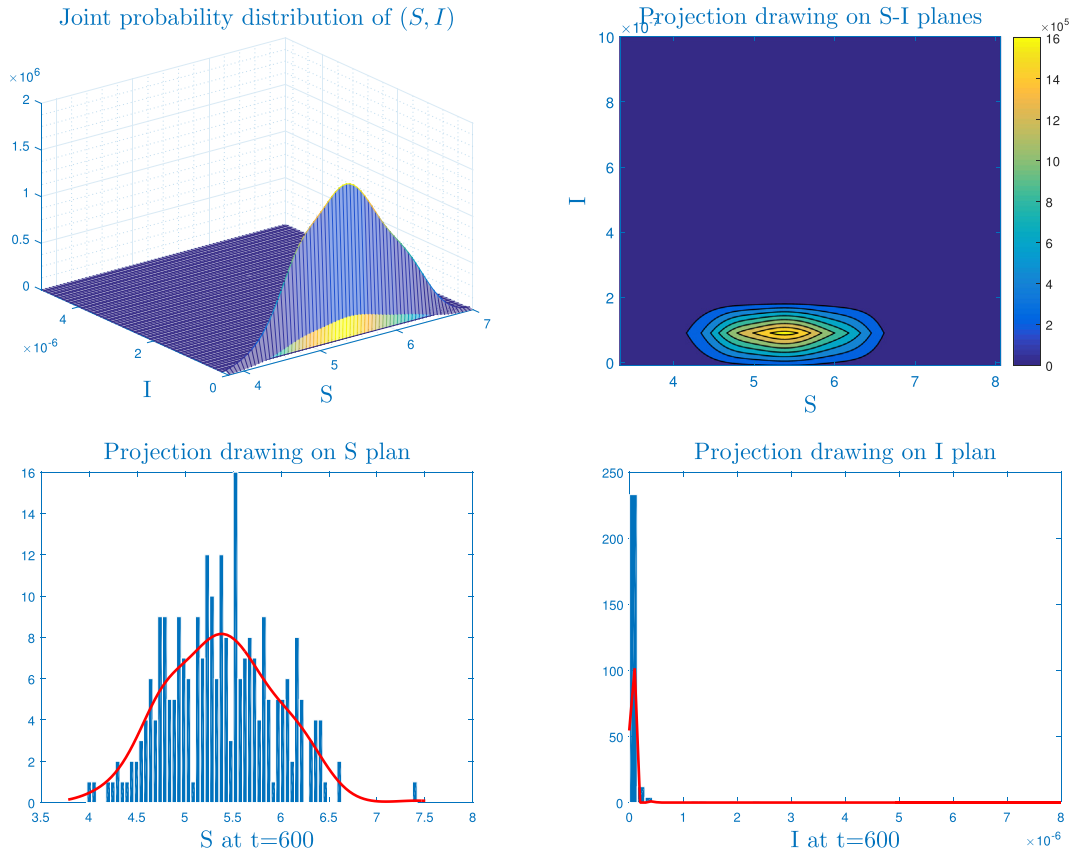

Fig. 8. Probability density function of (S,I) and its projection drawing on different coordinate planes. The deterministic parameters are selected from Table 1 - Test 3. For other noise intensities, we select $\xi_{11} = 0.1, \xi_{21} = 0.1, \xi_{12} = 0.1, \xi_{22} = 0.1, \chi_{11} = 0.15, \chi_{21} = 0.17, \chi_{12} = 0.12, \chi_{22} = 0.12$. In this case, $\mathcal{T}_0^\star = -0.0131 < 0$.

we show that COVID-19 persists continuously in the deterministic case. That is, the deterministic model (system (1.4) without noises) reaches the following stable steady point:

$$P^\star = (S^\star, I^\star, C^\star) = \left(\frac{\Pi}{\eta_d \mathcal{R}_0}, \frac{\eta_d}{\tau_\beta}(\mathcal{R}_0 - 1), \frac{\varpi}{\tau_\beta}(\mathcal{R}_0 - 1)\right) = (2.3391, 2.0099, 0.8614),$$

where $R_0 = \frac{\tau_\beta S^\star}{\eta_d + \eta_\alpha + \varpi} = 2.3208 > 1$. Now, by including random effects, we observe the permanence of the stochastic paths of system (1.4). Therefore, and by using real data, we interpret the strong persistence of COVID-19 in Morocco in the situation of high physical contact between individuals ($\tau_\beta = 0.23$). This is due to the lifting of the lock-down strategy in Morocco after summer of 2020 which leads to some jumps in the number of infected people. This last fact reinforces our consideration of Lévy noises in our model. On the other hand, we sketch experimental two-dimensional densities of $(S(t), I(t), C(t))$ in Fig. 2 in order to give a good overview of the stationarity property.

Obviously, the endemic equilibrium $P^\star$ of the corresponding deterministic version is no longer the steady state of the stochastic model (1.4). Therefore, in the following, we will numerically explore how the solutions of the stochastic model (1.4) behave around the deterministic equilibrium. For a sufficiently large time, we will calculate the time average of quantities $S(t)$, $I(t)$, and $C(t)$, for different noise intensities, and we discuss the asymptotic behaviors around $P^\star$. From Table 2, we observe that the intensity of linear white noise affects the fluctuation of the solution around the equilibrium. By way of explanation, the time average is close to $P^\star$ when the noise intensities are low. Most importantly, as noise intensity increases, the time-average of susceptible and recovered individuals raises, while the time-average of the infected population reduces. This phenomenon is observed for all types of noise with some variations (see Tables 3, 4, 5). Therefore, this fact illustrates the need to clearly integrate the influence of environmental fluctuations in the phenomenological description of biological systems. It is already clear that the quadratic fluctuations can explain the generalized effect of the worsening of the epidemiological situation, but in certain critical cases, the quadratic noise drastically affects the time extinction of the disease (we will discuss this case in Test 2).

In fact, noise is responsible for noise-induced transitions such that a stationary probability density function can suddenly change shape at certain noise intensity values (we will discuss this case in Test 3). From Remark 2.1, we mentioned that the explicit stationary distribution of a one-dimensional random differential equation with Lévy jumps is unknown. Same thing for a multidimensional systems. So, in this situation, we cannot analytically calculate the probability density function of some quantities during the transient dynamics. For a more physical understanding of the effect of noises on the shape of the density function (in the persistence case), we talk about the dispersion phenomenon. Explicitly, we plot the upper view of the joint density of the solution with some different values of white noises. Obviously, as the white noises increases, the distribution of the solution to system (1.4) will become more dispersed (see Fig. 3 (linear case) and Fig. 4 (quadratic case)).

4.1.2. Test 2: disappearance of COVID-19

Due to some intervention strategies to inhibit the spread of COVID-19 like lock-down, media coverage and vaccination, it makes sense that some parameters would be changed. In fact, these public health interventions are essential for minimizing the infection, but some measures are not really sufficiently functional when applied on their own and could not contain the outbreak. Multiple intrusions (like media coverage and vaccination) must be applied together in order to control the

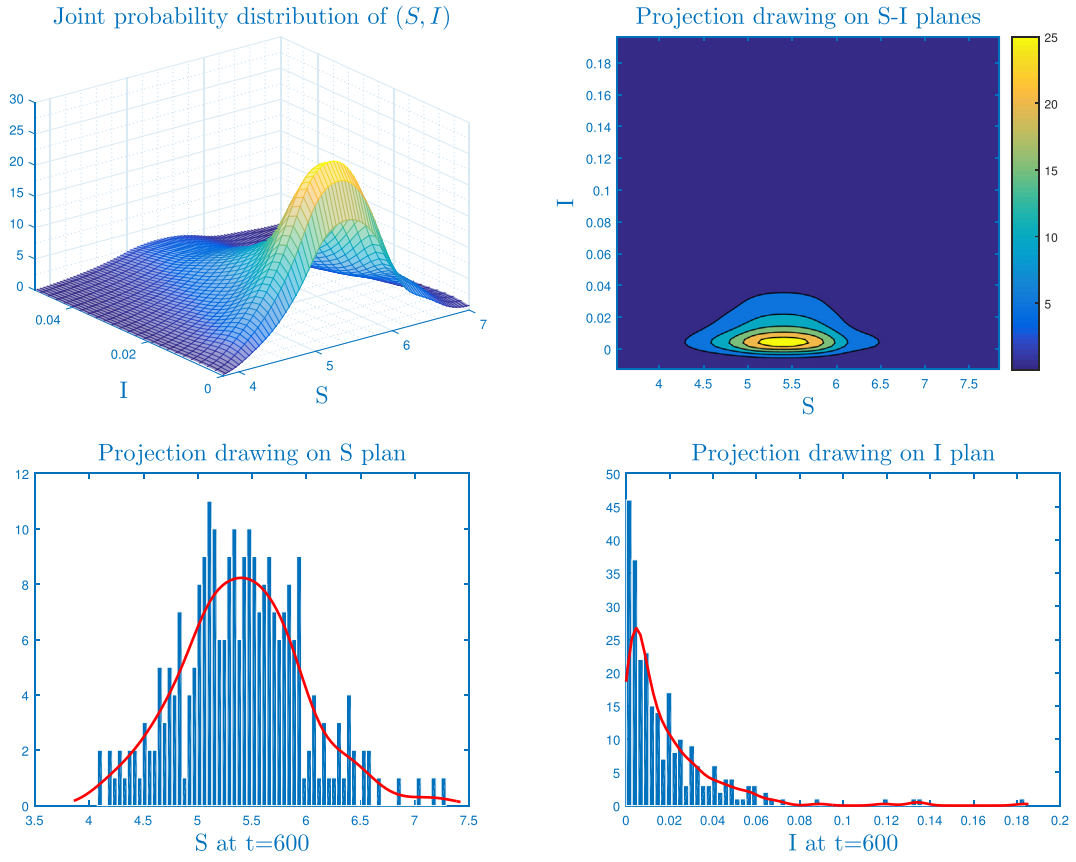

Fig. 9. Probability density function of (S,I) and its projection drawing on different coordinate planes. The deterministic parameters are selected from Table 1 - Test 3. For other noise intensities, we select $\xi_{11} = 0.01$, $\xi_{21} = 0.09710056563$, $\xi_{12} = 0.1$, $\xi_{22} = 0.1$, $\chi_{11} = 0.15$, $\chi_{21} = 0.017$, $\chi_{12} = 0.12$, $\chi_{22} = 0.12$. In this case, $\mathcal{T}_0^\star = 7.3284 \times 10^{-13} \approx 0$.

outbreak. For this reason, we theoretically consider a slight application of these strategies and we choose the values of the parameters from Table 1- Test 2. Concerning linear noises, we select $\xi_{11} = 0.08$, $\xi_{21} = 0.02$, $\xi_{31} = 0.07$, $\xi_{12} = 0.043$, $\xi_{22} = 0.043$, $\xi_{32} = 0.043$, $\chi_{11} = 0.15$, $\chi_{21} = 0.17$, $\chi_{31} = 0.11$, $\chi_{12} = 0.075$, $\chi_{22} = 0.075$, $\chi_{32} = 0.075$. A simple calculation gives

$$\mathcal{T}_0^\star = \frac{\tau_\beta \Pi}{\eta_d} - (\eta_d + \eta_\alpha + \varpi) - 0.5\xi_{21}^2 - \int_{\mathcal{H}} (\chi_{21}(u) - \ln(1 + \chi_{21}(u)))\vartheta(du) = -1.9625 \times 10^{-4} < 0.$$

Theoretical result check: according to Theorem 3.1, COVID-19 goes to extinction exponentially with probability one, and its deteriorate ratio constant is at least $\mathcal{T}_0^\star$.

Interpretation: epidemiologically, if the physical contact between individuals is minimized, the infection will disappear in the population. Specifically, if the transmission rate reaches at most 0.1015, we need 200 days for COVID-19 to disappear under some random factors of course. This randomness has a huge impact on the extinction time of COVID-19. Since quadratic noise do not appear in the threshold value, we explore its influence on the duration of infection. From Figs. 5 and 6, we emphasize that strong fluctuations (especially quadratic) have a passive influence on the time extinction of the disease. To illustrate the convergence of the distribution of the stochastic process $S(t)$ to that of $\Phi(t)$, we offer Fig. 7. Note that we have theoretically chosen the value of τ_β to get a threshold value close to zero, which makes us properly examine the sharpness of our threshold $\mathcal{T}_0^\star$.

4.1.3. Test 3: stochastic phenomenological bifurcation (SP-bifurcation)

In the above two subsections, we have studied numerically the dynamical bifurcation (D-bifurcation), which is caused by the abrupt change in the sign of the threshold $\mathcal{T}_0^\star$. In this part, we will explore the stochastic phenomenological bifurcation (SP-bifurcation), which principally depends on the abrupt change in the shape of the stationary probability density function of the model (1.6). Explicitly, we will show that the joint stationary probability density function of the classes S and I abruptly changes its shape at some values of the noise intensity. Firstly, we take deterministic parameter values from Table 1 - Test 3, and stochastic noise intensities as follows: $\xi_{11} = 0.1$, $\xi_{21} = 0.1$, $\xi_{12} = 0.1$, $\xi_{22} = 0.1$, $\chi_{11} = 0.15$, $\chi_{21} = 0.17$, $\chi_{12} = 0.12$, $\chi_{22} = 0.12$. Then, we get $\mathcal{T}_0^\star = -0.0131 < 0$. From Fig. 8, we plot the joint probability density function of (S,I) and its projection drawing on S and I planes. Plainly, we show the extinction of the class I and we remark that larger noise is not conducive to the continuation of the infection. Now, we keep the deterministic parameter values unchanged, and we select the stochastic noise intensities as follows: $\xi_{11} = 0.01$, $\xi_{21} = 0.09710056563$, $\xi_{12} = 0.1$, $\xi_{22} = 0.1$, $\chi_{11} = 0.15$, $\chi_{21} = 0.017$, $\chi_{12} = 0.12$, $\chi_{22} = 0.12$. In this situation, we obtain $\mathcal{T}_0^\star = 7.3284 \times 10^{-13}$ which is very very close to zero. In fact, the case of $\mathcal{T}_0^\star = 0$ is an absorbing state and the conditions of extinction and persistence of the infection are not so clear from physical point of view (see Fig. 9). Now we make slight changes to the stochastic noise intensities as follows: $\xi_{11} = 0.01$, $\xi_{21} = 0.09$, $\xi_{12} = 0.1$, $\xi_{22} = 0.1$, $\chi_{11} = 0.15$, $\chi_{21} = 0.017$, $\chi_{12} = 0.12$, $\chi_{22} = 0.12$. Then, we have $\mathcal{T}_0^\star = 6.6426 \times 10^{-4} > 0$ and we observe a significant change in the shape of the joint density function which is illustrated in Fig. 10. To more depict this, we decrease the amplitude of noises as follows: $\xi_{11} = 0.01$, $\xi_{21} = 0.01$, $\xi_{12} = 0.01$, $\xi_{22} = 0.01$, $\chi_{11} = 0.015$, $\chi_{21} = 0.017$, $\chi_{12} = 0.012$, $\chi_{22} = 0.012$. In this case, $\mathcal{T}_0^\star = 0.0029 > 0$. From Figs. 9–11, we can find that there is a sudden change for the probability density function at some values of the noise intensities. For a weak stochastic intensities: $\xi_{11} = 0.001$, $\xi_{21} = 0.001$, $\xi_{12} = 0.001$, $\xi_{22} = 0.001$, $\chi_{11} = 0.001$, $\chi_{21} =$

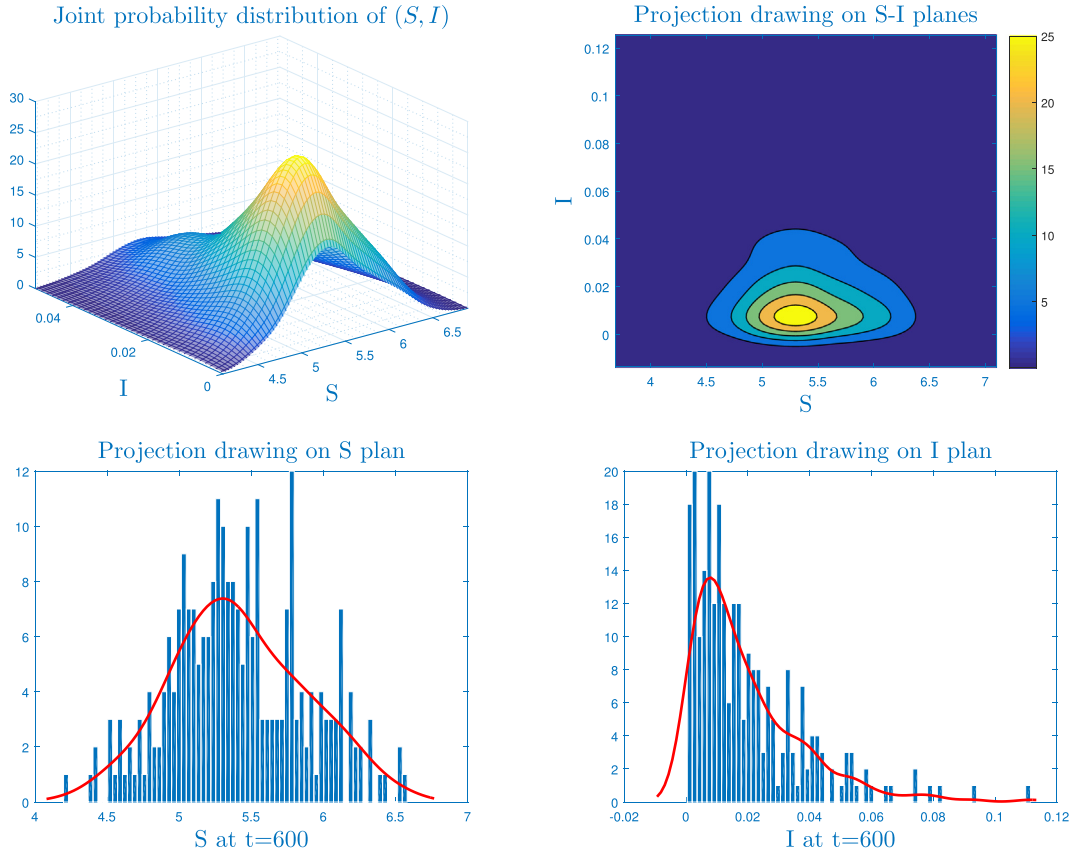

Fig. 10. Probability density function of (S,I) and its projection drawing on different coordinate planes. The deterministic parameters are selected from Table 1 - Test 3. For other noise intensities, we select $\xi_{11} = 0.01$, $\xi_{21} = 0.09$, $\xi_{12} = 0.1$, $\xi_{22} = 0.1$, $\chi_{11} = 0.15$, $\chi_{21} = 0.017$, $\chi_{12} = 0.12$, $\chi_{22} = 0.12$. In this case, $\mathcal{T}_0^\star = 6.6426 \times 10^{-4} > 0$.

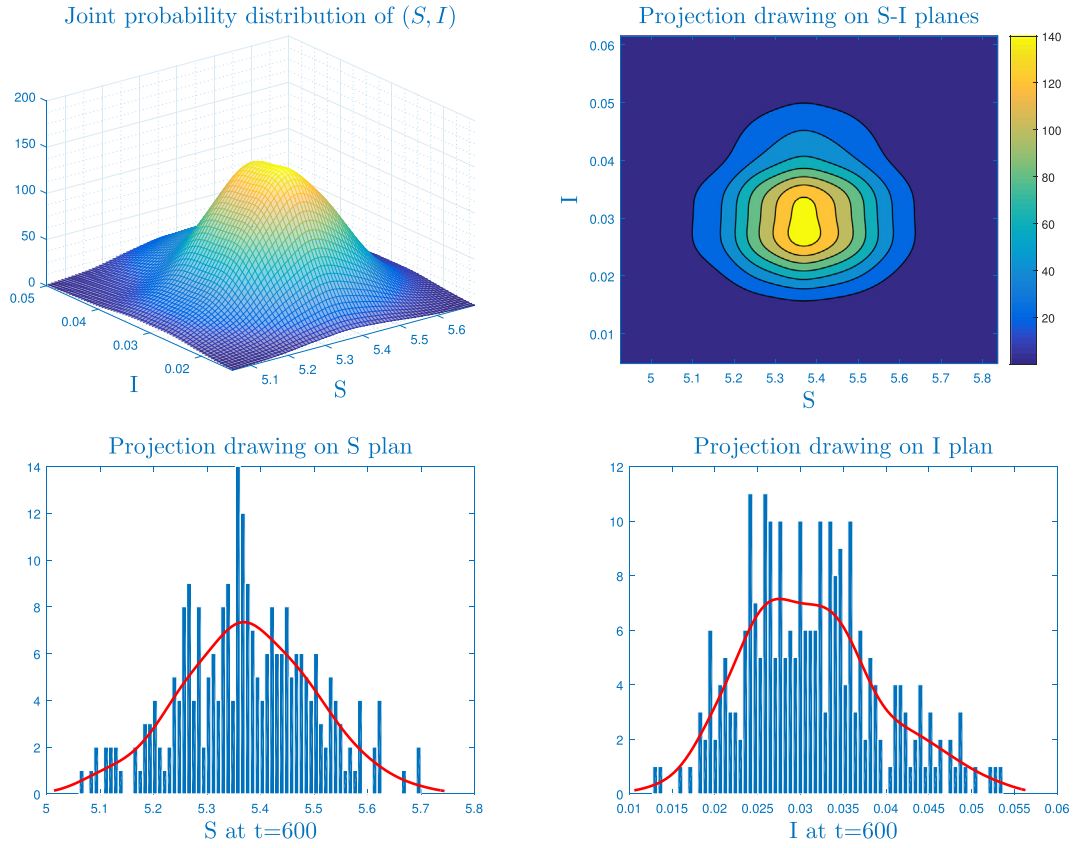

Fig. 11. Probability density function of (S,I) and its projection drawing on different coordinate planes. The deterministic parameters are selected from Table 1 - Test 3. For other noise intensities, we select $\xi_{11} = 0.01$, $\xi_{21} = 0.01$, $\xi_{12} = 0.01$, $\xi_{22} = 0.01$, $\chi_{11} = 0.015$, $\chi_{21} = 0.017$, $\chi_{12} = 0.012$, $\chi_{22} = 0.012$. In this case, $\mathcal{T}_0^\star = 0.0029 > 0$.

0.001, $\chi_{12} = 0.001$, $\chi_{22} = 0.001$, we get, $\mathcal{T}_0^\star = 0.0049 > 0$, and the shape of the density of (S,I) is depicted in Fig. 12. That is, the system (1.6) is strongly persistent.

4.2. Discussion

Environmental factors and unexpected phenomena have significant impacts on the spread of epidemics. This paper takes into account these two factors with quadratic representation. Specifically, we have analyzed an SIC epidemic model that incorporates quadratic Lévy jumps. Compared to previous works, many authors have considered the quadratic white noise perturbation (without Lévy jumps) in the various kinds of systems [75,94–96]. But there are some limitations of these papers, which can be explained as:

1. The complex and brutal random fluctuations are simulated by the white noise or Lévy jumps?
2. Can we obtain the exact value of the threshold between extinction and persistence?
3. Are the techniques and analysis presented in mentioned papers general for other stochastic models?

For this purpose, this study is dedicated to presenting a new general setting and to answer the above questions. Accurately,

1. We have mentioned (in the introduction) that in the majority of real and concrete situations, external disturbances are not continuous. For this, we have used the stochastic model with Lévy jumps.
2. Using the ergodic characteristic of the auxiliary system (2.1), the probabilistic comparison result, and the Lyapunov function approach, we have provided the sufficient and necessary criterion for the extinction and ergodicity of the distributed system (1.4). We indicate that the critical case $\mathcal{T}_0^\star = 0$ is still an open question that we will treat in the future. It is interesting to highlight that the state of $\mathcal{T}_0^\star = 0$ is an absorbed state and that the conditions for extinction and persistence of contagion are not very clear from a physical point of view
3. In this study, we have given the exact value of $\mathcal{T}_0^\star$. It is obvious that the linear noise intensities ξ_{21} and $\chi_{21}(u)$ have a passive influence on its value, and the quadratic noise quantities have no effect on it.
4. To prove the ergodicity, we have presented a novel technique that joins the Lyapunov method with the analysis used in [53].

To illustrate the sharpness of our results, we have performed some numerical simulations and we have confirmed that the impact of quadratic jumps on the threshold value is negligible. However, the nonlinearity hypothesis has a positive effect on the disease in the permanence case.

Generally speaking, we point out that this paper extends the study presented in [71] to the case of quadratic Lévy jumps and delivers some new insights for understanding the propagation of diseases with complex fluctuations. In other words, the proposed approach leaves many research paths to be explored in future works.

Concerning the exact expression of the probability density function of a stochastic system (1.4), we mention that this density obeys a non-local Fokker–Planck equation, difficult to solve analytically. Alternatively, we can obtain estimates of the probability density function through some numerical methods. In subsection 4.1.3, we have analyzed the effect of noises on the probability density function. We have concluded that its shape is changed at certain noise intensity values. This phenomenon requires more theoretical investigations. We will address this idea in our next investigation.

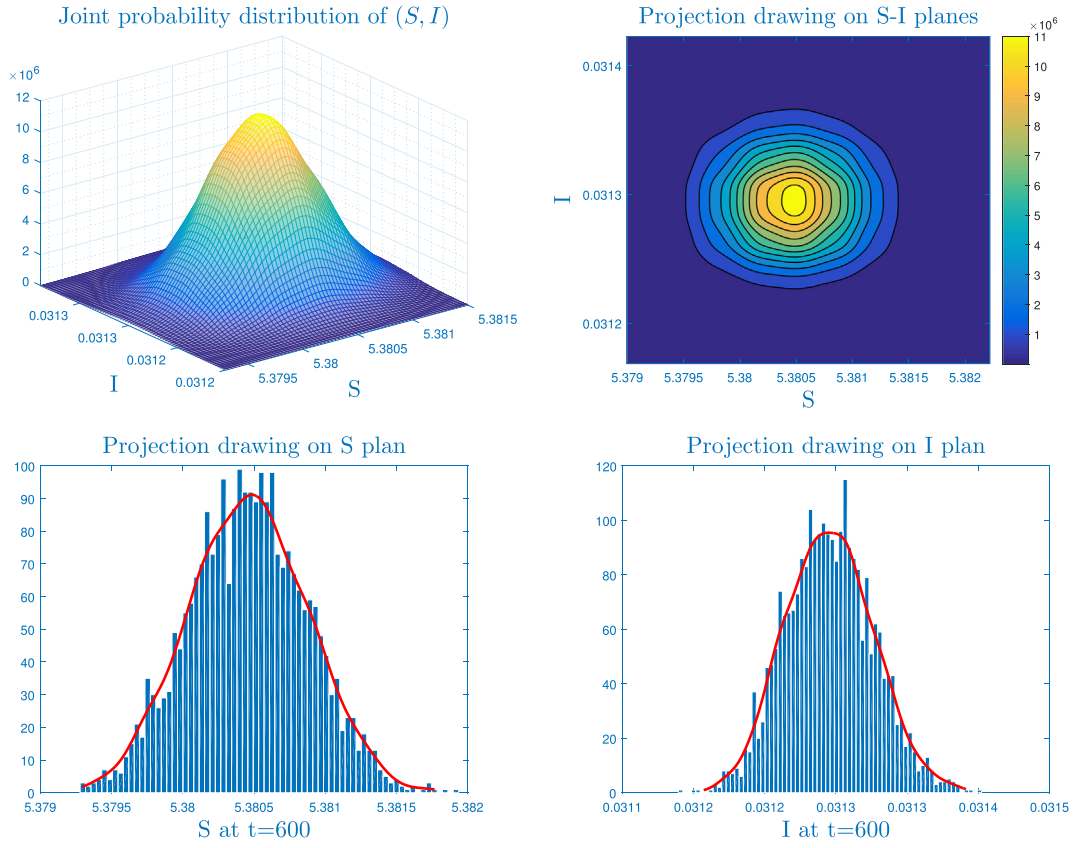

Fig. 12. Probability density function of (S,I) and its projection drawing on different coordinate planes. The deterministic parameters are selected from Table 1 - Test 3. For other noise intensities, we select $\xi_{11} = 0.01$, $\xi_{21} = 0.001$, $\xi_{12} = 0.001$, $\xi_{22} = 0.001$, $\chi_{11} = 0.001$, $\chi_{21} = 0.001$, $\chi_{12} = 0.001$, $\chi_{22} = 0.001$. In this case, $\mathcal{T}_0^\star = 0.0049 > 0$.

Declaration of competing interest

The authors declare that they have no known competing financial interests or personal relationships that could have appeared to influence the work reported in this paper.

Acknowledgement

The authors express their gratitude to the editor and expert reviewers for their comments and suggestions. The first author warmly thanks Professor Sanling Yuan (Shanghai, China) for his clarifications.

Funding

This work was supported by the Science and Engineering Research Board (SERB) of India (EEQ/2021/001003).

Data availability

The real and theoretical data used to support the findings of this study are already included in the article.

CRediT authorship contribution statement

Yassine Sabbar: Writing – original draft, Formal analysis, Investigation, Conceptualization, Methodology, Software. **Driss Kiouach**: Methodology, Investigation, Writing – review and editing. **S.P. Rajasekar**: Conceptualization, Investigation, Writing - reviewing and editing. **Salim El Azami El-idrissi**: Review.

References

[1] Kermack WO, McKendrick AG. A contribution to the mathematical theory of epidemics. ProcRSocA MathPhysEngSci. 1927;115(772):700–21.
[2] Heymann DL, Shindo N. COVID-19: what is next for public health? Lancet. 2020;395 (10224):542–5.
[3] Hossain M. The effect of the COVID-19 on sharing economy activities. J Clean Prod. 2021;280(1):124782.
[4] Z. Wang K. Tang , "Combating COVID-19: health equity matters," Nature Medicine, vol. 26, no. 4, p. 485.
[5] Azizi H, Esmaeili ED. Challenges and potential solutions in the development of COVID-19 pandemic control measuresl. New MicrobesNew Infect. 2021;40:100852.
[6] Brodin P. Immune determinants of COVID-19 disease presentation and severity. Nat Med. 2021;27:28–33.
[7] Neufeld Z, Khataee H, Czirok A. Targeted adaptive isolation strategy for COVID-19 pandemic. InfectDisModel. 2020;5:357–61.
[8] Buonomo B. Effects of information-dependent vaccination behavior on coronavirus outbreak: insights from a SIRI model. RicercheMatematica. 2020;69(2):483–99.
[9] Anderson RM, May RM. Population biology of infectious diseases: part I. Nature. 1979;280(5721):361–7.
[10] Roy M, Holt RD. Effects of predation on host-pathogen dynamics in SIR models. Theor Popul Biol. 2008;73(3):319–31.
[11] Guo H, Li MY, Shuai Z. Global stability of the endemic equilibrium of multigroup SIR epidemic models. CanApplMathQ. 2006;14(3):259–84.
[12] Prodanov D. Analytical parameter estimation of the SIR epidemic model. Applications to the COVID-19 pandemic. Entropy. 2021;23(1):59.
[13] Kudryashov NA, Chmykhov MA, Vigdorowitsch M. Analytical features of the SIR model and their applications to COVID-19. App Math Model. 2021;90:466–73.
[14] Abdy M, Side S, Annas S, Nur W, Sanusi W. An sir epidemic model for covid-19 spread with fuzzy parameter: the case of Indonesia. AdvDifferEqu. 2021.;105.
[15] Tornatore E, Buccellato SM, Vetro P. Stability of a stochastic SIR system. PhysA. 2005; 354:111–26.
[16] Kiouach D, Sabbar Y. Stability and threshold of a stochastic SIRS epidemic model with vertical transmission and transfer from infectious to susceptible individuals. DiscretDynNatSoc. 2018;2018:7570296.
[17] Horsthemke W, Lefever R. Noise-induced transitions: theory and applications in physics, chemistry, and biology. Springer; 1984..

[18] Ciuchi S, De Pasquale F, Spagnolo B. Nonlinear relaxation in the presence of an absorbing barrier. PhysRevE. 1993;47(6):3915.
[19] Ciuchi S, De Pasquale F, Spagnolo B. Self-regulation mechanism of an ecosystem in a non-Gaussian fluctuation regime. PhysRevE. 1996;54(1):706.
[20] Denaro G, Valenti D, Spagnolo B, Basilone G, Mazzola S, Zgozi SW, Aronica S, Bonanno A. Dynamics of two picophytoplankton groups in Mediterranean sea: analysis of the deep chlorophyll maximum by a stochastic advection-reaction-diffusion model. PLoS One. 2013;8(6):e66765.
[21] Caruso A, Gargano ME, Valenti D, Fiasconaro A, Spagnolo B. Cyclic fluctuations, climatic changes and role of noise in planktonic foraminifera in the Mediterranean sea. FluctuationNoise Lett. 2005;5(2):L349–55.
[22] Spagnolo B, Cirone M, La Barbera A, De Pasquale F. Noise-induced effects in population dynamics. J Phys Condens Matter. 2002;14(9):2247.
[23] Spagnolo B, La Barbera A. Role of the noise on the transient dynamics of an ecosystem of interacting species. PhysA. 2002;315:114–24.
[24] Guarcello C, Valenti D, Spagnolo B. Phase dynamics in graphene-based Josephson junctions in the presence of thermal and correlated fluctuations. PhysRevB. 2015; 92(17):174519.
[25] Guarcello C, Valenti D, Carollo A, Spagnolo B. Stabilization effects of dichotomous noise on the lifetime of the superconducting state in a long Josephson junction. Entropy. 2015;17(5):2862–75.
[26] Carollo A, Valenti D, Spagnolo B. Geometry of quantum phase transitions. Phys Rep. 2020;838:1–72.
[27] Ushakov YV, Dubkov AA, Spagnolo B. Spike train statistics for consonant and dissonant musical accords in a simple auditory sensory model. PhysRevE. 2010;81 (4):041911.
[28] Yakimov AV, Filatov DO, Gorshkov ON, Antonov DA, Liskin DA, Antonov IN, Belyakov AV, Klyuev AV, Carollo A, Spagnolo B. Measurement of the activation energies of oxygen ion diffusion in yttria stabilized zirconia by flicker noise spectroscopy. Appl Phys Lett. 2019;114(25):253506.
[29] Mikhaylov A, Pimashkin A, Pigareva Y, Gerasimova S, Gryaznov E, Shchanikov S, Zuev A, Talanov M, Lavrov I, Demin V, Erokhin V, Lobov S, Mukhina I, Kazantsev V, Wu H, Spagnolo B. Neurohybrid memristive CMOS-integrated systems for biosensors and neuroprosthetics. Front Neurosci. 2020;14:358.
[30] Carollo A, Spagnolo B, Valenti D. Uhlmann curvature in dissipative phase transitions. Sci Rep. 2018;8(1):1–16.
[31] Xu C, Yuan S, Zhang T. Competitive exclusion in a general multi-species chemostat model with stochastic perturbations. Bull Math Biol. 2021;83(1):1–17.
[32] Zhang S, Zhang T, Yuan S. Dynamics of a stochastic predator-prey model with habitat complexity and prey aggregation. EcolComplex. 2021;45:100889.
[33] Yang A, Song B, Yuan S. Noise-induced transitions in a non-smooth SIS epidemic model with media alert. Math Biosci Eng. 2021;18(1):745–63.
[34] Yan S, Yuan S. Critical value in a SIR network model with heterogeneous infectiousness and susceptibility. Math Biosci Eng. 2020;17(5):5802–11.
[35] Shaikhet L. Stability of stochastic differential equations with distributed and state-dependent delays. JApplMathComput. 2020;4(4):181–8.
[36] Shaikhet L. Improving stability conditions for equilibria of SIR epidemic model with delay under stochastic perturbations. Mathematics. 2020;8(8):1302.
[37] Bunimovich-Mendrazitsky S, Shaikhet L. Stability analysis of delayed tumor-antigen-activated immune response in combined BCG and IL-2 immunotherapy of bladder cancer. Processes. 2020;8(12):1564.
[38] Bentout S, Chen Y, Djilali S. Global dynamics of an SEIR model with two age structures and a nonlinear incidence. Acta ApplicMath. 2021;171(1):1–27.
[39] Rajasekar SP, Pitchaimani M. Ergodic stationary distribution and extinction of a stochastic sirs epidemicmodel with logistic growth and nonlinear incidence. Appl Math Comput. 2020;377:125143.
[40] Rajasekar SP, Pitchaimani M, Zhu Q. Progressive dynamics of a stochastic epidemic model with logistic growth and saturated treatment. PhysA. 2019;538:122649.
[41] Rajasekar SP, Pitchaimani M, Zhu Q, Shi K. Exploring the stochastic host-pathogen tuberculosis model with adaptive immune response. Math Probl Eng. 2021.;2021.
[42] May RM. Stability and complexity in model ecosystems. Princeton Landmarks in Biology; 2001..
[43] Ji C, Jiang D, Shi N. The behavior of an SIR epidemic model with stochastic perturbation. Stochastic AnalApplic. 2012;30(5):755–73.
[44] Ji C, Jiang D. Threshold behaviour of a stochastic SIR model. App Math Model. 2014; 38(21):5067–79.
[45] Jiang D, Yu J, Ji C, Shi N. Asymptotic behavior of global positive solution to a stochastic SIR model. MathComputModell. 2011;45(1):221–32.
[46] Lin Y, Jiang D, Xia P. Long-time behavior of a stochastic SIR model. Appl Math Comput. 2014;236:1–9.
[47] Djilali S, Benahmadi L, Tridane A, Niri K. Modeling the impact of unreported cases of the COVID-19 in the North African countries. Biology. 2020;9(11):373.
[48] Bentout S, Tridane A, Djilali S, Touaoula TM. Age-structured modeling of COVID-19 epidemic in the USA, UAE and Algeria. Alex Eng J. 2021;60(1):401–11.
[49] Pitchaimani M, Brasanna DM. Stochastic dynamical probes in a triple delayed SICR model with general incidence rate and immunization strategies. Chaos, SolitonsFractals. 2021;143:110540.
[50] Rajasekar SP, Pitchaimani M, Zhu Q. Dynamic threshold probe of stochastic SIR model with saturated incidence rate and saturated treatment function. PhysA. 2019;535:122300.
[51] Khan A, Hussain G, Zahri M, Zaman G. A stochastic SACR epidemic model for HBV transmission. J Biol Dyn. 2020;14(1):788–801.
[52] Hussain G, Khan A, Zahri M, Zaman G. Stochastic permanence of an epidemic model with a saturated incidence rate. Chaos SolitonsFractals. 2020;139:110005.
[53] Zhao D, Yuan S. Sharp conditions for the existence of a stationary distribution in one classical stochastic chemostat. Appl Math Comput. 2018;339:199–205.
[54] Zhang XB, Shi Q, Ma SH, Huo H, Li D. Dynamic behavior of a stochastic SIQS epidemic model with levy jumps. Nonlinear Dyn. 2018;93(3):1481–93.
[55] Chichigina O, Dubkov AA, Valenti D, Spagnolo B. Stability in a system subject to noise with regulated periodicity. PhysRevE. 2011;84(2):021134.
[56] Chichigina O, Valenti D, Spagnolo B. A simple noise model with memory for biological systems. FluctuationNoise Lett. 2005;5(2):L243–50.
[57] Zhang X, Wang K. Stochastic SIR model with jumps. ApplMathLett. 2013;26(8): 867–74.
[58] Zhou Y, Zhang W. Threshold of a stochastic SIR epidemic model with Levy jumps. PhysA. 2016;446:204–2016.
[59] Zhao D, Yuan S, Liu H. Stochastic dynamics of the delayed chemostat with Levy noises. Int J Biomath. 2019.;12(5).
[60] Kiouach D, Sabbar Y, El-idrissi SEA. New results on the asymptotic behavior of an SIS epidemiological model with quarantine strategy, stochastic transmission, and Levy disturbance. MathMethodsApplSci. 2021;44(17):13468–92.
[61] Kiouach D, Sabbar Y. Developing new techniques for obtaining the threshold of a stochastic SIR epidemic model with 3-dimensional Levy process. JApplNonlinear Dyn. 2022;11(2):401–14.
[62] Kiouach D, Sabbar Y. The long-time behaviour of a stochastic SIR epidemic model with distributed delay and multidimensional Levy jumps. IntJBiomath. 2021;2021: 2250004.
[63] Kiouach D, Sabbar Y. Dynamic characterization of a stochastic sir infectious disease model with dual perturbation. IntJBiomath. 2021;14(4):2150016.
[64] Kiouach D, Sabbar Y. Ergodic stationary distribution of a stochastic hepatitis B epidemic model with interval-valued parameters and compensated Poisson process. Comput Math Methods Med. 2020;2020:9676501.
[65] Gihman II, Skorohod AV. Stochastic differential equations. Berlin Heidelberg: Springer; 1972..
[66] Cheng Y, Zhang F, Zhao M. A stochastic model of HIV infection incorporating combined therapy of Haart driven by levy jumps. AdvDifferEqu. 2019;2019(1):1–17.
[67] Cheng Y, Li M, Zhang F. A dynamics stochastic model with HIV infection of CD4 T cells driven by levy noise. Chaos, SolitonsFractals. 2019;129:62–70.
[68] Gao M, Jiang D, Hayat T, Alsaedi A. Threshold behavior of a stochastic Lotka Volterra food chain chemostat model with jumps. PhysA. 2019;523:191–203.
[69] Li S, Guo S. Persistence and extinction of a stochastic sis epidemic model with regime switching and levy jumps. DiscretContinDynSystB. 2021;26(9):5101.
[70] Akdim K, Ez-zetouni A, Danane J, Allali K. Stochastic viral infection model with lytic and nonlytic immune responses driven by levy noise. PhysA. 2020;549:124367.
[71] Dieu NT, Fugo T, Du NH. Asymptotic behaviors of stochastic epidemic models with jump-diffusion. App Math Model. 2020;86:259–70.
[72] Privault N, Wang L. Stochastic sir levy jump model with heavy tailed increments. JNonlinear Sci. 2021;31(1):1–28.
[73] Guarcello C, Valenti D, Carollo A, Spagnolo B. Effects of levy noise on the dynamics of sine-Gordon solitons in long Josephson junctions. JStatMechTheoryExp. 2016; 2016:054012.
[74] Guarcello C, Valenti D, Spagnolo B, Pierro V, Filatrella G. Anomalous transport effects on switching currents of graphene-based Josephson junctions. Nanotechnology. 2017;28(13):134001.
[75] Liu Q, Jiang D, Hayat T, Ahmed B. Periodic solution and stationary distribution of stochastic SIR epidemic models with higher order perturbation. PhysA. 2017;482: 209–17.
[76] Rajasekar SP, Pitchaimani M, Zhu Q. Higher order stochastically perturbed SIRS epidemic model with relapse and media impact. MathMethodsApplSci. 2022;45: 843–63.
[77] Liu Q, Jiang D. Stationary distribution and extinction of a stochastic SIR model with nonlinear perturbation. ApplMathLett. 2017;73:8–15.
[78] Liu Q, Jiang D, Hayat T, Ahmed B. Stationary distribution and extinction of a stochastic predator-prey model with additional food and nonlinear perturbation. Appl Math Comput. 2018;320:226–39.
[79] Lv X, Meng X, Wang X. Extinction and stationary distribution of an impulsive stochastic chemostat model with nonlinear perturbation. Chaos, SolitonsFractals. 2018;110:273–9.
[80] Zhou Y, Zhang W, Yuan S. Survival and stationary distribution of a SIR epidemic model with stochastic perturbations. Appl Math Comput. 2014;244:118–31.
[81] Lv J, Liu H, Zou X. Stationary distribution and persistence of a stochastic predator-prey model with a functional response. JApplAnalComput. 2019;9(1):1–11.
[82] Peng S, Zhu X. Necessary and sufficient condition for comparison theorem of 1-dimensional stochastic differential equations. StochProcessApplic. 2006;116(3): 370–80.
[83] Dieu NT, Nguyen DH, Du NH, Yin G. Classification of asymptotic behavior in a stochastic SIR model. SIAM JApplDynSyst. 2016;15(2):1062–84.
[84] Zhang X, Yang Q. Dynamical behavior of a stochastic predator-prey model with general functional response and nonlinear jump-diffusion. DiscretContinDynSystB. 2021;vol:2021.
[85] Kutoyants YA. Statistical inference for ergodic diffusion processes. London, UK: Springer; 2004..
[86] Xi F. Asymptotic properties of jump-diffusion processes with state-dependent switching. StochProcessApplic. 2009;119(7):2198–221.
[87] Mao X. Stochastic differential equations and applications. Chichester: Elsevierl; 2007..
[88] Khasminskii R. Stochastic stability of differential equations. , 66Springer Science and Business Media; 2011..
[89] Stettner L. On the existence and uniqueness of invariant measure for continuous-time markov processes. province, RI: LCDS, Brown University; 1986. p. 18–86. Technical Report.

[90] Tong J, Zhang Z, Bao J. The stationary distribution of the facultative population model with a degenerate noise. StatProbabLett. 2013;83(2):655–64.
[91] S. of health ministry of Morocco. www.sante.gov.ma, www.covidmaroc.ma; 2021. 2021.
[92] Danane J, Allali K, Hammouch Z, Nizar KS. Mathematical analysis and simulation of a stochastic COVID-19 levy jump model with isolation strategy. ResultsPhys. 2021; 23:103994.
[93] Liberati NB, Platen E. Strong approximations of stochastic differential equations with jumps. JComputApplMath. 2007;205(2):982–1001.
[94] Han B, Zhou B, Jiang D, Hayat T, Alsaedi A. Stationary solution, extinction and density function for a high-dimensional stochastic SEI epidemic model with general distributed delay. Appl Math Comput. 2021.;405(126236).
[95] Lu C, Sun G, Zhang Y. Stationary distribution and extinction of a multi-stage HIV model with nonlinear stochastic perturbation. JApplMathComput. 2021;2021:1–23.
[96] Liu Q. Dynamics of a stochastic sica epidemic model for HIV transmission with higher-order perturbation. StochAnalApplic. 2021;2021:1–40.